

Detecting light axions from supernovae in nearby galaxies

Francesca Lecce ^{1,2,*} Alessandro Lella ^{1,2,†} Giuseppe Lucente ^{3,‡} Maurizio Giannotti ^{4,5,§} and Alessandro Mirizzi ^{1,2,¶}

¹*Dipartimento Interuniversitario di Fisica “Michelangelo Merlin”, Via Amendola 173, 70126 Bari, Italy*

²*Istituto Nazionale di Fisica Nucleare - Sezione di Bari, Via Orabona 4, 70126 Bari, Italy*

³*SLAC National Accelerator Laboratory, 2575 Sand Hill Rd, Menlo Park, CA 94025*

⁴*Centro de Astropartículas y Física de Altas Energías, University of Zaragoza, Zaragoza, 50009, Aragón, Spain*

⁵*Physical Sciences, Barry University, 11300 NE 2nd Ave., Miami Shores, FL 33161, USA*

(Dated: December 5, 2025)

Axion-like particles (ALPs) coupled to nucleons can be efficiently produced in core-collapse supernovae (SNe) and then, if they couple to photons, convert into gamma rays in cosmic magnetic fields, generating short gamma-ray bursts. Though ALPs from a Galactic SN would induce an intense and easily detectable gamma-ray signal, such events are exceedingly rare. In contrast, a few SNe per year are expected in nearby galaxies within $\sim \mathcal{O}(10)$ Mpc, where strong magnetic fields can enable more efficient ALP–photon conversions than in the Milky Way, offering a promising extragalactic target. This circumstance motivates full-sky gamma-ray monitoring, ideally combined with deci-hertz gravitational-wave detectors to enable time-triggered searches from nearby galaxies. We show that, under realistic conditions, a decade of coverage could reach sensitivities to ALP-photon coupling $g_{a\gamma} \gtrsim 10^{-16} \text{ GeV}^{-1}$ for ALP masses $m_a \lesssim 10^{-9} \text{ eV}$ and assuming an ALP-nucleon coupling close to SN 1987A cooling bound. This sensitivity would allow one to probe a large, currently-unexplored region of the parameter space below the longstanding SN 1987A bound.

Introduction.— Axion-like particles (ALPs) emerge in several extensions of the Standard Model of particle physics [1–6]. From a top-down perspective, string theory predicts the presence of an “axiverse” with the QCD axion [7–10] and several ultralight ALPs [11–13]. From a bottom-up perspective, ALPs offer an interesting physics case in relation to dark matter [14–18] and several astrophysical puzzles [19–22]. In this context, stars provide ideal environments for ALP production due to their hot, dense plasmas [23, 24] (see Refs. [25, 26] for recent reviews). The Sun, being the closest star to Earth, has been extensively studied using “helioscope” experiments [27–29] and X-ray detectors [30]. Nevertheless, other stellar systems offer competitive discovery potential [26].

Remarkably, following the detection of neutrinos from Supernova SN 1987A [31–35], it was proposed that ALPs could be copiously produced in the supernova (SN) core alongside neutrinos [36, 37]. In particular, a substantial ALP flux can be generated via interactions with nucleons in the hot and dense SN core [36, 38–40]. If also coupled with photons, a fraction of these ALPs could convert into gamma rays in the Milky Way magnetic field, yielding a short gamma-ray burst coincident with the neutrino signal. The absence of such a signal in the Gamma-Ray Spectrometer aboard the Solar Maximum Mission led to stringent constraints on the product of the ALP-proton and ALP-photon couplings [41–46], excluding $g_{ap} \times g_{a\gamma} \gtrsim 3.6 \times 10^{-24} \text{ GeV}^{-1}$ for $m_a \lesssim 10^{-10} \text{ eV}$ (see the gray band in Fig. 1).

The observation of a future Galactic core-collapse supernova (CCSN) would enable tests of substantially smaller ALP couplings [51–53]. For example, if the *Fermi* Large Area Telescope (LAT) were to

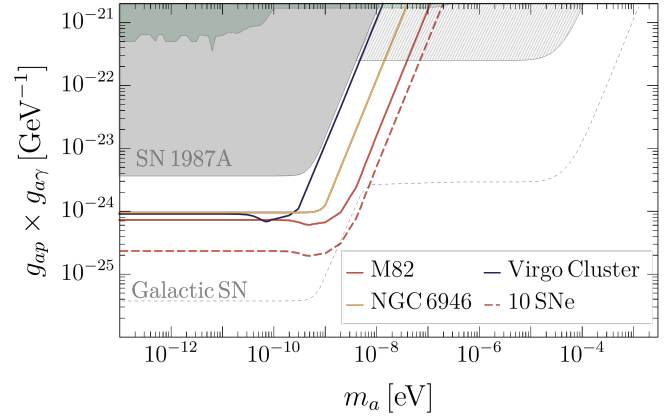


FIG. 1. Sensitivities at 95% CL in the $g_{ap} \times g_{a\gamma}$ vs m_a plane for future extragalactic SN occurring in M82 (red), NGC 6946 (yellow) or Virgo Cluster (black) for a *Fermi*-LAT-like gamma-ray detector, assuming an observation time window of $\Delta t = 10 \text{ s}$ enabled by the core-collapse time trigger provided by deci-hertz GW interferometers. The dashed red curve illustrates the stacked sensitivity from 10 SNe in an environment similar to M82. The gray band displays the constraint from the non-observation of gamma rays from SN 1987A for ALPs converting in the Milky-Way, while the hatched region would be probed by conversions in the SN 1987A progenitor magnetosphere assuming a 100 G surface field [45], but no measurements of such field are available [46]. For comparison, we also show the sensitivity to a future Galactic SN at a distance of $d = 10 \text{ kpc}$ (dashed black curve) by assuming the same magnetic field models used for the SN 1987A limit. Finally, we show in green the dominant astrophysical bounds in this mass range [47–50].

observe such a SN event, it could probe down to $g_{ap} \times g_{a\gamma} \gtrsim 3.7 \times 10^{-26} \text{ GeV}^{-1}$ for ultra-light ALPs with $m_a \ll 10^{-9} \text{ eV}$ (see the dashed black curve in Fig. 1). In addition, including ALP–photon conversions in the strong magnetic field of the progenitor star may even grant access to the canonical QCD axion parameter space [45, 46, 54]. Though all this sounds extremely promising, Galactic SNe are rare events, occurring at a rate of only about two per century [55].

A different approach consists in the observation of individual extragalactic SNe, producing ALPs that convert in gamma-rays within the Milky Way magnetic field.

This idea was first explored in Ref. [56], which investigated the sensitivity of *Fermi*-LAT to extragalactic events, at a distance $d \lesssim 270 \text{ Mpc}$. However, unlike Galactic SNe, the core-collapse time cannot be precisely determined because neutrino bursts from such distances are undetectable with current and near-future underground experiments [57]. In the absence of a neutrino trigger, the explosion time must be inferred from the optical light curves [58]. This substantially enlarges the observational time window during which ALP-induced gamma rays may appear, transforming an otherwise background-free search into a background-dominated one. Additionally, the limited field of view of *Fermi*-LAT may prevent coverage at the relevant core-collapse time (see Ref. [59] for a discussion of how the probability that *Fermi*-LAT observes at least one SN at the time of collapse scales with the sample size).

For this reason, extragalactic SNe have remained largely off the radar. The aim of this Letter is to show that this picture can change dramatically if forthcoming experimental proposals are realized. Furthermore, nearby galaxies may host magnetic environments in which the probabilities of ALP-photon conversion are enhanced by 2–3 orders of magnitude relative to the Milky Way [49, 60, 61]. With the proper experimental setup, extragalactic SNe could become a genuinely transformative tool, allowing us to probe ALP parameter space far beyond current limits (see Fig. 1).

ALPs from extragalactic SNe: What is needed?— To clarify the physics case for ALP searches from extragalactic SNe, in Fig. 2 we plot the number of observed CCSN rate up to a distance $d = 20 \text{ Mpc}$ reported in the Transient Name Server [62] for the period 2008–2025, corresponding to the lifetime of *Fermi*-LAT. The detailed list of core-collapse SNe with their distances is reported in the Supplemental Material (SM A). From such a plot, one infers that roughly seven core-collapse SNe per year occurred within this volume. Therefore, extending the SN horizon to nearby galaxies dramatically increases the number of potential events, removing the dependence on the rare occurrence of a Galactic SN. Based on these results, in this Letter we show that to turn extragalactic CCSNe into powerful ALP laboratories, two key experimental capabilities are required: (a) a

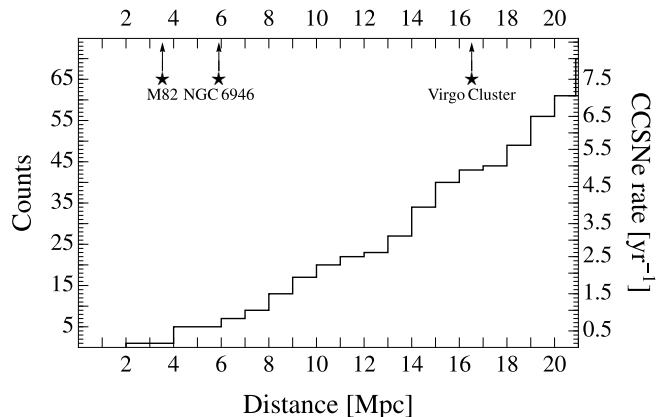


FIG. 2. Cumulative number of observed core-collapse supernovae in the period 2008–2025 (left vertical axis) from nearby galaxies in function of the distance. On the right vertical axis is also indicated the inferred SN rate per year.

full-sky, continuously operating constellation of gamma-ray detectors; (b) an external time trigger that determines the SN core-collapse time with sufficient accuracy. These are not speculative or serendipitous conditions—they represent clear, achievable technological objectives whose realization would decisively enable extragalactic ALP astrophysics. The first objective, condition (a), is well within reach. Concepts such as the GALAXIS mission [45] already outline a satellite constellation with *Fermi*-LAT-like sensitivity and genuine full-sky coverage. Although primarily designed for Galactic SNe, we show below that its physics reach extends naturally to extragalactic distances when combined with requirement (b).

This latter prerequisite is equally realistic. While large underground neutrino detectors are intrinsically limited to probing SNe within a few Mpc [57], current optical surveys, which aim to discover SNe up to tens of Mpc, may determine the core-collapse time with an accuracy of $\Delta t = 1 \text{ d}$ [63, 64]. Furthermore, future optical surveys, may reach $\Delta t = 1 \text{ h}$ [58]. Indeed, by modeling the early light curve of the SN, Ref. [65] determined the core-collapse time of real SNe within an accuracy of better than a few hours. Finally, next-generation deci-hertz GW observatories (DECIGO, BBO) [66–68] are expected to detect the supernova gravitational *neutrino-memory* signal out to tens of Mpc [57, 69], providing the optimal explosion-time trigger needed for ALP searches. Building on these possibilities, we show that the presence of an accurate external trigger may open new regions of ALP parameter space beyond those excluded by SN 1987A observations.

ALP production in SN core.— The production of ALPs in the SN core has been extensively studied over the past decades [23, 36, 39, 46, 70–73]. A particularly efficient production channel is nucleon–nucleon (NN) bremsstrahlung [39], mediated

by the ALP–nucleon interaction described by the Lagrangian $\mathcal{L}_{aN} = (2m_N)^{-1} \partial_\mu a \sum_{N=p,n} g_{aN} \bar{N} \gamma^\mu \gamma_5 N$, where a is the ALP field, m_N is the nucleon mass, and g_{aN} is the ALP coupling to nucleon species, with $N = p, n$ for protons and neutrons, respectively. In the following, for simplicity, we assume ALPs coupling only to protons. In this work we calculate the SN ALP fluxes using as benchmark the 1D spherical symmetric GARCHING group’s SN model SFHo-s18.8 provided in Ref. [74] and based on the neutrino-hydrodynamics code PROMETHEUS-VERTEX [75]. Notably, the NN bremsstrahlung produces an ALP thermal spectrum with average energy $E_a \simeq 70$ MeV. The emissivity can be further enhanced if a sizable population of thermal pions is present in the SN core, enabling additional ALP production through pionic Compton-like (πN) processes [40]. Due to the uncertainties in this process, we neglect it in the following discussion. See the SM B for more details on the SN ALP emissivity.

ALP-photon conversions in host galaxies.— Generically, ALPs can also couple to photons through the Lagrangian term [76, 77], $\mathcal{L}_{a\gamma} = g_{a\gamma} a \mathbf{E} \cdot \mathbf{B}$, where $g_{a\gamma}$ is the ALP-photon coupling. In this scenario, ultralight ALPs would efficiently convert within the cosmic magnetic fields, giving rise to a gamma-ray signal observable by gamma-ray experiments operating in the MeV energy range. In Ref. [56] the conversions of ALPs from extragalactic SNe were characterized by assuming only the presence of the Milky Way magnetic field. Therefore, compared to the case of a Galactic SN at $d \sim 10$ kpc, we expect a flux penalty factor for extragalactic SNe $\mathcal{O}([10 \text{ kpc}/10 \text{ Mpc}]^2) \sim 10^{-6}$, leading to a reduction in the sensitivity to $g_{ap} \times g_{a\gamma}$ of three orders of magnitudes. However, the penalty associated with the much larger distances of extragalactic SNe can be substantially mitigated by the presence of strong magnetic fields in and around their host galaxies. As recently shown in Ref. [49], ALPs produced in stellar populations of nearby galaxies can undergo highly efficient conversions in these environments. A particularly striking example is the M82 starburst galaxy ($d = 3.5$ Mpc), where magnetic fields enhanced by starburst activity can reach ~ 0.1 – 1 mG [78], leading to sizable ALP–photon conversion probabilities [49, 60, 61].¹ Ref. [49] also examined the elliptical galaxy M87 ($d = 16.9$ Mpc). The latter would benefit from its position inside the Virgo Cluster, where Mpc-scale intracluster magnetic fields provide long conversion baselines that can compensate the inherently weaker strengths. Following Ref. [49], we model the B -field and the electron density in these environments using the cosmological magnetohydrodynamical simulations from ILLUSTRISTNG [80, 81], as documented in

the SM C. As an additional example, we consider a third system, the spiral galaxy NGC 6946 at $d = 5.9$ Mpc. Although relatively small ($L \sim 9$ kpc), it hosts magnetic fields of order $\mathcal{O}(10) \mu\text{G}$ [82]. This case is particularly useful for assessing the impact of using ILLUSTRISTNG data in our conversion-probability estimates. For NGC 6946, we directly compared the TNG-based predictions with those obtained from the dedicated spiral magnetic-field model of Ref. [82], supplemented with electron densities from Ref. [83]. The resulting conversion probabilities differ by less than a factor of two, confirming the robustness of our approach (see SM C for further details about the computation of conversion probabilities).

In order to calculate ALP-photon conversions, we closely follow the technique described in Ref. [84], to which we address the reader for more details. For each subhalo modeling the properties of the environment, we compute the conversion probabilities along 1000 random lines of sight and we define our *fiducial* line of sight the one associated with the average conversion probability. This latter for $g_{a\gamma} = 10^{-12} \text{ GeV}^{-1}$ assumes values $P_{a\gamma} = 7.7 \times 10^{-3}$ for M82, $P_{a\gamma} = 1.2 \times 10^{-2}$ for NGC 6946, and $P_{a\gamma} = 1.1 \times 10^{-1}$ for Virgo Cluster, in the limit of $m_a \lesssim 10^{-9}$ eV. The observed gamma-ray flux will scale as $\Phi_\gamma \propto P_{a\gamma}/d^2$, implying $\Phi_\gamma^{\text{M82}} : \Phi_\gamma^{\text{NGC 6946}} : \Phi_\gamma^{\text{M87}} = 1 : 0.5 : 0.6$. Therefore, despite the differences in the input parameters, one expects a similar sensitivity to $g_{ap} \times g_{a\gamma}$ as shown in Fig. 1. Furthermore, we highlight that typical values of the conversion probability in the Milky Way are $P_{a\gamma} \sim \mathcal{O}(10^{-5})$ for $g_{a\gamma} = 10^{-12} \text{ GeV}^{-1}$ and so negligible with respect to the values reached in all the considered environments. Indeed, accounting for conversions only in the Milky Way, for a SN exploding in M82 we would find a sensitivity to $g_{ap} \times g_{a\gamma} \sim 1.3 \times 10^{-23} \text{ GeV}^{-1}$, which is above the existing bound from SN 1987A. We also observe that the effect of a potentially strong magnetic field in the progenitor of the SN, as considered in [45, 46, 54], would extend the sensitivity to larger masses but in a region of the parameter space already excluded by other astrophysical constraints. Therefore, for simplicity we neglect also this effect.

Sensitivities in $g_{ap} \times g_{a\gamma}$.— With these results in hand, we are ready to derive the sensitivity to the product of ALP–nucleon and ALP–photon couplings $g_{ap} \times g_{a\gamma}$. Since the three nearby galaxies introduced before are expected to give a similar sensitivity in the low-mass ALP range ($m_a \lesssim 10^{-9}$ eV), for definiteness we focus on M82. We assume to have a gamma-ray detector like the proposed project GALAXIS [45] with the same performances of *Fermi*-LAT, guaranteeing full sky coverage (see SM D for details). In Fig. 3, we show the 95% confidence level (CL) sensitivity [85] to $g_{ap} \times g_{a\gamma}$ in case of low-mass ALPs assuming different observation-time windows, determined by the accuracy in the determination of the SN core-collapse time. In low-background regime,

¹ Observations of this galaxy also allow constraints on massive ALPs decaying into photons [79].

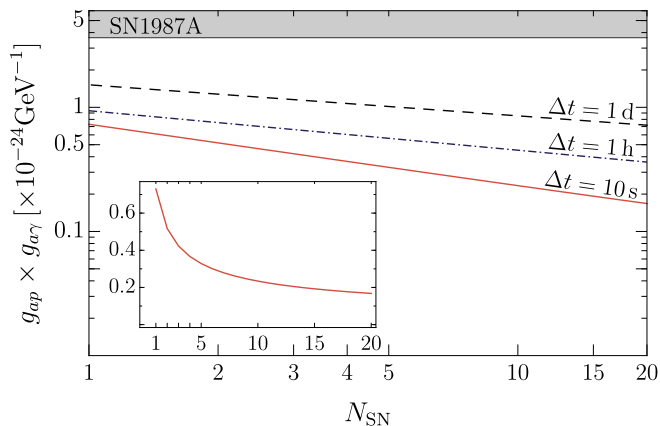


FIG. 3. Sensitivity (95% CL) on $g_{ap} \times g_{a\gamma}$ as a function of the number of observed extragalactic SNe, N_{SN} , yielding a gamma-ray flux similar to the one estimated in the case of M82. We assume different time windows to search for the ALP signal, namely $\Delta t = 1$ d (dashed curve), $\Delta t = 1$ h (dot-dashed curve), $\Delta t = 10$ s (continuous curve). In the inset we show on a linear scale the sensitivity for $\Delta t = 10$ s scaling as $N_{\text{SN}}^{-1/2}$. The x and y axes are the same as in the main panel.

the statistical analysis follows the Feldman–Cousins prescription [86].

As a first case, we consider an accuracy of $\Delta t = 1$ d (dashed curve) determined by the extrapolation of the observed lightcurve from optical surveys [63, 64]. In such a large observational time window the gamma-ray detector is expected to accumulate a significant number of background events [$N_{\text{bkg}} \sim \mathcal{O}(100)$]. Therefore, the statistical analysis points out that if a SN explodes in M82, we will be sensitive to $g_{ap} \times g_{a\gamma} \gtrsim 1.5 \times 10^{-24} \text{ GeV}^{-1}$ at 95% CL, which is a factor 2.4 below the SN 1987A bound.

In this case, the significant improvement expected with respect to the results of Ref. [56] is due to enhancement of the conversions in the magnetic environment of the host galaxy with respect to the Milky-Way, as shown in SM F.

In order to further improve the sensitivities, it is crucial to reduce the background shortening the uncertainty on the determination of the SN core-collapse time. Let us first assume that future optical surveys might be able to reach $\Delta t = 1$ h (dot-dashed curve), as considered in Ref. [58]. With this accuracy, we get a sensitivity of $g_{ap} \times g_{a\gamma} \gtrsim 9.4 \times 10^{-25} \text{ GeV}^{-1}$, improving by a factor ~ 1.6 the case with $\Delta t = 1$ d. Finally, we consider the optimistic scenario of $\Delta t = 10$ s (continuous curve) corresponding to the duration of the ALP burst. Achieving such a narrow observational window requires a precise determination of the burst onset, expected to be possible in the presence of a deci-Hertz GW interferometer observing the SN neutrino memory signal. In this case, since we are in a background-free regime, we compute the 95% CL

sensitivity by requiring that ~ 3 ALP-induced events are observed [86], leading to $g_{ap} \times g_{a\gamma} \gtrsim 7.3 \times 10^{-25} \text{ GeV}^{-1}$. This corresponds to an improvement over the SN 1987A bound by a factor ~ 5 .

We also estimate how the sensitivity would improve if multiple extragalactic SN explosions are observed over the detector’s lifetime. From the SN catalog covering the period 2008–2025 (Table S1 in SM A), we find that seven SNe occurred during this time window in the three environments considered in this work (see Table S3). Since the expected ALP-induced signal from each of these systems is comparable to that of M82, observing seven such events is effectively equivalent to detecting seven explosions from M82 itself. Therefore, we show in Fig. 3 the resulting sensitivity enhancement as a function of the number of observed SNe N_{SN} , adopting M82 as a benchmark case. In a background-dominated situation, corresponding to SN core-collapse time known with an accuracy of $\Delta t = 1$ d, the sensitivity to $g_{ap} \times g_{a\gamma}$ scales as $N_{\text{SN}}^{-1/4}$. For $\Delta t = 1$ h, one finds an intermediate regime between background-free and high-background scenarios.

Short coincidence windows, $\Delta t \approx 10$ s, enabled by a GW trigger, suppress the expected background and can place the search in the background-free regime. Besides the obvious advantages of a reduced background, in this limit stacking becomes maximally efficient, with the coupling sensitivity scaling as $g_{ap} g_{a\gamma} \propto N_{\text{SN}}^{-1/2}$. Thus, reducing the time window directly accelerates the gain from multiple events. This provides strong motivation for synergies with next-generation GW detectors, which can sharply localize the burst time. As an illustration, stacking $N_{\text{SN}} = 5$ core-collapse SNe within $d \simeq 20$ Mpc, each with an M82-like expected flux, yields a projected sensitivity of $g_{ap} \times g_{a\gamma} \simeq 3.3 \times 10^{-25} \text{ GeV}^{-1}$, an improvement of almost one order of magnitude over the SN 1987A bound. Remarkably, this corresponds to $g_{a\gamma} \gtrsim 10^{-16} \text{ GeV}^{-1}$, assuming $g_{ap} \sim 10^{-9}$ (near the SN 1987A cooling limit [46, 73]). Beyond ~ 10 stacked extragalactic SNe, however, the returns become marginal, as shown in the inset of Fig. 3. Consequently, even with a rate of one nearby SN per year, a decade-long monitoring program would be sufficient to either detect a signal or set a substantially stronger bound on the ALP couplings.

Conclusions.— Core-collapse supernovae in nearby galaxies offer a powerful and previously underutilized opportunity to explore the ALP parameter space well beyond existing limits. Their unique role stems from the fact that several nearby galaxies host magnetic environments—ranging from starburst-driven mG fields to cluster-scale intracluster structures—where ALP–photon conversion efficiencies exceed those of the Milky Way by 2–3 orders of magnitude.

In addition, few core-collapse SNe are expected to occur every year within ~ 20 Mpc, providing a steady

stream of potential ALP sources. Yet current gamma-ray facilities lack the full-sky coverage and time-tagging accuracy needed to exploit these events effectively. Our analysis shows that two realistic experimental capabilities would decisively change this situation: (i) a full-sky, continuously operating constellation of MeV gamma-ray detectors, and (ii) an external trigger capable of determining the core-collapse time to within seconds, most naturally provided by next-generation deci-hertz GW interferometers. If these conditions are met, extragalactic SNe become a transformative ALP probe. A single explosion in a favorable host galaxy would surpass the SN 1987A constraint, and a decade-long program could explore $g_{ap} \times g_{a\gamma}$ at the level of $\sim 10^{-25} \text{ GeV}^{-1}$, reaching deep into currently inaccessible parameter space.

Extragalactic SN ALP searches would thus represent a major new frontier in *multi-messenger astronomy*. By combining gamma rays, optical surveys, and gravitational waves, they open a realistic pathway toward *extragalactic ALP astronomy*, in which the cumulative SN activity of the local universe becomes a precision tool for fundamental physics.

Acknowledgments—We warmly thank Damiano F.G. Fiorillo, Orion Ning, and Edoardo Vitagliano for their helpful comments on the manuscript. This article is based on work from COST Action COSMIC WISPerS CA21106, supported by COST (European Cooperation in Science and Technology). The work of AM and AL and FL was partially supported by the research grant number 2022E2J4RK ”PANTHEON: Perspectives in Astroparticle and Neutrino THEory with Old and New messengers” under the program PRIN 2022 (Mission 4, Component 1, CUP I53D23001110006) funded by the Italian Ministero dell’Università e della Ricerca (MUR) and by the European Union – Next Generation EU. GL acknowledges support from the U.S. Department of Energy under contract number DE-AC02-76SF00515. This work is (partially) supported by ICSC – Centro Nazionale di Ricerca in High Performance Computing. MG acknowledges support from the Spanish Agencia Estatal de Investigación under grant PID2019-108122GB-C31, funded by MCIN/AEI/10.13039/501100011033, and from the “European Union NextGenerationEU/PRTR” (Planes complementarios, Programa de Astrofísica y Física de Altas Energías). He also acknowledges support from grant PGC2022-126078NB-C21, “Aún más allá de los modelos estándar,” funded by MCIN/AEI/10.13039/501100011033 and “ERDF A way of making Europe.” Additionally, MG acknowledges funding from the European Union’s Horizon 2020 research and innovation programme under the European Research Council (ERC) grant agreement ERC-2017-AdG788781 (IAXO+).

* francesca.lecce@ba.infn.it

† alessandro.lella@ba.infn.it

‡ lucenteg@slac.stanford.edu

§ mgiannotti@unizar.es

¶ alessandro.mirizzi@ba.infn.it

- [1] J. Jaeckel and A. Ringwald, *The Low-Energy Frontier of Particle Physics*, *Ann. Rev. Nucl. Part. Sci.* **60** (2010) 405 [1002.0329].
- [2] A. Ringwald, *Axions and Axion-Like Particles*, in *49th Rencontres de Moriond on Electroweak Interactions and Unified Theories*, pp. 223–230, 2014, 1407.0546.
- [3] L. Di Luzio, M. Giannotti, E. Nardi and L. Visinelli, *The landscape of QCD axion models*, *Phys. Rept.* **870** (2020) 1 [2003.01100].
- [4] P. Agrawal et al., *Feebly-interacting particles: FIPs 2020 workshop report*, *Eur. Phys. J. C* **81** (2021) 1015 [2102.12143].
- [5] M. Giannotti, *Aspects of Axions and ALPs Phenomenology*, *J. Phys. Conf. Ser.* **2502** (2023) 012003 [2205.06831].
- [6] C. Antel et al., *Feebly-interacting particles: FIPs 2022 Workshop Report*, *Eur. Phys. J. C* **83** (2023) 1122 [2305.01715].
- [7] R. D. Peccei and H. R. Quinn, *CP Conservation in the Presence of Instantons*, *Phys. Rev. Lett.* **38** (1977) 1440.
- [8] R. D. Peccei and H. R. Quinn, *Constraints Imposed by CP Conservation in the Presence of Instantons*, *Phys. Rev. D* **16** (1977) 1791.
- [9] S. Weinberg, *A New Light Boson?*, *Phys. Rev. Lett.* **40** (1978) 223.
- [10] F. Wilczek, *Problem of Strong P and T Invariance in the Presence of Instantons*, *Phys. Rev. Lett.* **40** (1978) 279.
- [11] A. Arvanitaki, S. Dimopoulos, S. Dubovsky, N. Kaloper and J. March-Russell, *String Axiverse*, *Phys. Rev. D* **81** (2010) 123530 [0905.4720].
- [12] M. Cicoli, M. Goodsell and A. Ringwald, *The type IIB string axiverse and its low-energy phenomenology*, *JHEP* **10** (2012) 146 [1206.0819].
- [13] M. Cicoli, J. P. Conlon, A. Maharana, S. Parameswaran, F. Quevedo and I. Zavala, *String cosmology: From the early universe to today*, *Phys. Rept.* **1059** (2024) 1 [2303.04819].
- [14] L. F. Abbott and P. Sikivie, *A Cosmological Bound on the Invisible Axion*, *Phys. Lett. B* **120** (1983) 133.
- [15] M. Dine and W. Fischler, *The Not So Harmless Axion*, *Phys. Lett. B* **120** (1983) 137.
- [16] J. Preskill, M. B. Wise and F. Wilczek, *Cosmology of the Invisible Axion*, *Phys. Lett. B* **120** (1983) 127.
- [17] P. Arias, D. Cadamuro, M. Goodsell, J. Jaeckel, J. Redondo and A. Ringwald, *WISPy Cold Dark Matter*, *JCAP* **06** (2012) 013 [1201.5902].
- [18] C. B. Adams et al., *Axion Dark Matter*, in *Snowmass 2021*, 3, 2022, 2203.14923.
- [19] M. Giannotti, I. Irastorza, J. Redondo and A. Ringwald, *Cool WISPs for stellar cooling excesses*, *JCAP* **05** (2016) 057 [1512.08108].
- [20] M. Giannotti, I. G. Irastorza, J. Redondo, A. Ringwald and K. Saikawa, *Stellar Recipes for Axion Hunters*, *JCAP* **10** (2017) 010 [1708.02111].

- [21] L. Di Luzio, M. Fedele, M. Giannotti, F. Mescia and E. Nardi, *Stellar evolution confronts axion models*, *JCAP* **02** (2022) 035 [2109.10368].
- [22] G. Galanti, L. Nava, M. Roncadelli, F. Tavecchio and G. Bonnoli, *Observability of the Very-High-Energy Emission from GRB 221009A*, *Phys. Rev. Lett.* **131** (2023) 251001 [2210.05659].
- [23] G. G. Raffelt, *Stars as laboratories for fundamental physics: The astrophysics of neutrinos, axions, and other weakly interacting particles*. 5, 1996.
- [24] G. G. Raffelt, *Particle physics from stars*, *Ann. Rev. Nucl. Part. Sci.* **49** (1999) 163 [hep-ph/9903472].
- [25] A. Caputo and G. Raffelt, *Astrophysical Axion Bounds: The 2024 Edition*, *PoS COSMICWISPerS* (2024) 041 [2401.13728].
- [26] P. Carena, M. Giannotti, J. Isern, A. Mirizzi and O. Straniero, *Axion astrophysics*, *Phys. Rept.* **1117** (2025) 1 [2411.02492].
- [27] K. van Bibber, P. M. McIntyre, D. E. Morris and G. G. Raffelt, *A Practical Laboratory Detector for Solar Axions*, *Phys. Rev. D* **39** (1989) 2089.
- [28] IAXO Collaboration, E. Armengaud et al., *Physics potential of the International Axion Observatory (IAXO)*, *JCAP* **06** (2019) 047 [1904.09155].
- [29] IAXO Collaboration, A. Abeln et al., *Conceptual design of BabyIAXO, the intermediate stage towards the International Axion Observatory*, *JHEP* **05** (2021) 137 [2010.12076].
- [30] J. Ruz et al., *NuSTAR as an Axion Helioscope*, *Phys. Rev. Lett.* **135** (2025) 141001 [2407.03828].
- [31] KAMIOKANDE-II Collaboration, K. Hirata et al., *Observation of a Neutrino Burst from the Supernova SN 1987a*, *Phys. Rev. Lett.* **58** (1987) 1490.
- [32] K. S. Hirata et al., *Observation in the Kamiokande-II Detector of the Neutrino Burst from Supernova SN 1987a*, *Phys. Rev. D* **38** (1988) 448.
- [33] E. N. Alekseev, L. N. Alekseeva, I. V. Krivosheina and V. I. Volchenko, *Detection of the Neutrino Signal From SN1987A in the LMC Using the Inr Baksan Underground Scintillation Telescope*, *Phys. Lett. B* **205** (1988) 209.
- [34] R. M. Bionta et al., *Observation of a Neutrino Burst in Coincidence with Supernova SN 1987a in the Large Magellanic Cloud*, *Phys. Rev. Lett.* **58** (1987) 1494.
- [35] IMB Collaboration, C. B. Bratton et al., *Angular Distribution of Events From Sn1987a*, *Phys. Rev. D* **37** (1988) 3361.
- [36] R. P. Brinkmann and M. S. Turner, *Numerical Rates for Nucleon-Nucleon Axion Bremsstrahlung*, *Phys. Rev. D* **38** (1988) 2338.
- [37] A. Burrows, M. S. Turner and R. P. Brinkmann, *Axions and SN 1987a*, *Phys. Rev. D* **39** (1989) 1020.
- [38] W. Keil, H.-T. Janka, D. N. Schramm, G. Sigl, M. S. Turner and J. R. Ellis, *A Fresh look at axions and SN-1987A*, *Phys. Rev. D* **56** (1997) 2419 [astro-ph/9612222].
- [39] P. Carena, T. Fischer, M. Giannotti, G. Guo, G. Martínez-Pinedo and A. Mirizzi, *Improved axion emissivity from a supernova via nucleon-nucleon bremsstrahlung*, *JCAP* **10** (2019) 016 [1906.11844]. [Erratum: JCAP 05, E01 (2020)].
- [40] P. Carena, B. Fore, M. Giannotti, A. Mirizzi and S. Reddy, *Enhanced Supernova Axion Emission and its Implications*, *Phys. Rev. Lett.* **126** (2021) 071102 [2010.02943].
- [41] J. A. Grifols, E. Masso and R. Toldra, *Gamma-rays from SN1987A due to pseudoscalar conversion*, *Phys. Rev. Lett.* **77** (1996) 2372 [astro-ph/9606028].
- [42] J. W. Brockway, E. D. Carlson and G. G. Raffelt, *SN1987A gamma-ray limits on the conversion of pseudoscalars*, *Phys. Lett. B* **383** (1996) 439 [astro-ph/9605197].
- [43] A. Payez, C. Evoli, T. Fischer, M. Giannotti, A. Mirizzi and A. Ringwald, *Revisiting the SN1987A gamma-ray limit on ultralight axion-like particles*, *JCAP* **02** (2015) 006 [1410.3747].
- [44] S. Hoof and L. Schulz, *Updated constraints on axion-like particles from temporal information in supernova SN1987A gamma-ray data*, *JCAP* **03** (2023) 054 [2212.09764].
- [45] C. A. Manzari, Y. Park, B. R. Safdi and I. Savoray, *Supernova Axions Convert to Gamma Rays in Magnetic Fields of Progenitor Stars*, *Phys. Rev. Lett.* **133** (2024) 211002 [2405.19393].
- [46] D. F. G. Fiorillo, Á. Gil Muyor, H.-T. Janka, G. G. Raffelt and E. Vitagliano, *Axion-photon conversion in transient compact stars: Systematics, constraints, and opportunities*, **2509.13322**.
- [47] C. O'Hare, *cajohare/axionlimits: Axionlimits*, <https://cajohare.github.io/AxionLimits/>, July, 2020. 10.5281/zenodo.3932430.
- [48] J. S. Reynés, J. H. Matthews, C. S. Reynolds, H. R. Russell, R. N. Smith and M. C. D. Marsh, *New constraints on light axion-like particles using Chandra transmission grating spectroscopy of the powerful cluster-hosted quasar H1821+643*, *Mon. Not. Roy. Astron. Soc.* **510** (2021) 1264 [2109.03261].
- [49] O. Ning and B. R. Safdi, *Leading Axion-Photon Sensitivity with NuSTAR Observations of M82 and M87*, *Phys. Rev. Lett.* **134** (2025) 171003 [2404.14476].
- [50] J. N. Benabou, C. Dessert, K. C. Patra, T. G. Brink, W. Zheng, A. V. Filippenko and B. R. Safdi, *Search for Axions in Magnetic White Dwarf Polarization at Lick and Keck Observatories*, **2504.12377**.
- [51] M. Meyer, M. Giannotti, A. Mirizzi, J. Conrad and M. A. Sánchez-Conde, *Fermi Large Area Telescope as a Galactic Supernovae Axionscope*, *Phys. Rev. Lett.* **118** (2017) 011103 [1609.02350].
- [52] F. Calore, P. Carena, C. Eckner, M. Giannotti, G. Lucente, A. Mirizzi and F. Sivo, *Uncovering axionlike particles in supernova gamma-ray spectra*, *Phys. Rev. D* **109** (2024) 043010 [2306.03925].
- [53] A. Lella, F. Calore, P. Carena, C. Eckner, M. Giannotti, G. Lucente and A. Mirizzi, *Probing protoneutron stars with gamma-ray axionscopes*, *JCAP* **11** (2024) 009 [2405.02395].
- [54] F. R. Candón, D. F. G. Fiorillo, Á. Gil Muyor, H.-T. Janka, G. G. Raffelt and E. Vitagliano, *Stripped-Envelope Supernovae for QCD Axion Detection*, **2511.13815**.
- [55] K. Rozwadowska, F. Vissani and E. Cappellaro, *On the rate of core collapse supernovae in the milky way*, *New Astron.* **83** (2021) 101498 [2009.03438].
- [56] M. Meyer and T. Petrushevska, *Search for Axionlike-Particle-Induced Prompt γ -Ray Emission from Extragalactic Core-Collapse Supernovae with the Fermi Large Area Telescope*, *Phys. Rev. Lett.* **124**

- (2020) 231101 [2006.06722]. [Erratum: Phys.Rev.Lett. 125, 119901 (2020)].
- [57] M. Mukhopadhyay, Z. Lin and C. Lunardini, *Memory-triggered supernova neutrino detection*, *Phys. Rev. D* **106** (2022) 043020 [2110.14657].
- [58] S. Heston, E. Kehoe, Y. Suwa and S. Horiuchi, *Timing coincidence search for supernova neutrinos with optical transient surveys*, *Phys. Rev. D* **107** (2023) 123034 [2302.04884].
- [59] F. R. Candón, D. F. G. Fiorillo, H.-T. Janka, B. F. A. van Baal and E. Vitagliano, *Small Progenitors, Large Couplings: Type Ic Supernova Constraints on Radiatively Decaying Particles*, **2509.18253**.
- [60] O. Ning and B. R. Safdi, *Probing the Axion-Electron Coupling with NuSTAR Observations of Galaxies*, **2503.09682**.
- [61] O. Ning, A. Ray and B. R. Safdi, *Axion lines from nuclear de-excitations in galactic stellar populations*, **2509.03569**.
- [62] A. Gal-Yam, *The TNS alert system*, in *American Astronomical Society Meeting Abstracts #237*, vol. 237 of *American Astronomical Society Meeting Abstracts*, p. 423.05, Jan., 2021.
- [63] S. Ando, J. F. Beacom and H. Yuksel, *Detection of neutrinos from supernovae in nearby galaxies*, *Phys. Rev. Lett.* **95** (2005) 171101 [astro-ph/0503321].
- [64] L. Tartaglia et al., *The early detection and follow-up of the highly obscured Type II supernova 2016ija/DLT16am*, *Astrophys. J.* **853** (2018) 62 [1711.03940].
- [65] D. Cowen, A. Franckowiak and M. Kowalski, *Estimating the explosion time of core-collapse supernovae from their optical light curves*, *Astroparticle Physics* **33** (2010) 19–23.
- [66] N. Seto, S. Kawamura and T. Nakamura, *Possibility of direct measurement of the acceleration of the universe using 0.1-Hz band laser interferometer gravitational wave antenna in space*, *Phys. Rev. Lett.* **87** (2001) 221103 [astro-ph/0108011].
- [67] K. Yagi and N. Seto, *Detector configuration of DECIGO/BBO and identification of cosmological neutron-star binaries*, *Phys. Rev. D* **83** (2011) 044011 [1101.3940]. [Erratum: Phys.Rev.D 95, 109901 (2017)].
- [68] S. Kawamura et al., *Current status of space gravitational wave antenna DECIGO and B-DECIGO*, *PTEP* **2021** (2021) 05A105 [2006.13545].
- [69] M. Mukhopadhyay, C. Cardona and C. Lunardini, *The neutrino gravitational memory from a core collapse supernova: phenomenology and physics potential*, *JCAP* **07** (2021) 055 [2105.05862].
- [70] M. Carena and R. D. Peccei, *The Effective Lagrangian for Axion Emission From SN1987A*, *Phys. Rev. D* **40** (1989) 652.
- [71] G. Raffelt and D. Seckel, *A selfconsistent approach to neutral current processes in supernova cores*, *Phys. Rev. D* **52** (1995) 1780 [astro-ph/9312019].
- [72] A. Lella, P. Carena, G. Lucente, M. Giannotti and A. Mirizzi, *Protoneutron stars as cosmic factories for massive axionlike particles*, *Phys. Rev. D* **107** (2023) 103017 [2211.13760].
- [73] A. Lella, P. Carena, G. Co', G. Lucente, M. Giannotti, A. Mirizzi and T. Rauscher, *Getting the most on supernova axions*, *Phys. Rev. D* **109** (2024) 023001 [2306.01048].
- [74] *Garching core-collapse supernova research archive*, <https://wwwmpa.mpa-garching.mpg.de/ccsnarchive//>.
- [75] M. Rampp and H. T. Janka, *Radiation hydrodynamics with neutrinos: Variable Eddington factor method for core collapse supernova simulations*, *Astron. Astrophys.* **396** (2002) 361 [astro-ph/0203101].
- [76] G. G. Raffelt and D. S. P. Dearborn, *Bounds on Hadronic Axions From Stellar Evolution*, *Phys. Rev. D* **36** (1987) 2211.
- [77] G. Raffelt and L. Stodolsky, *Mixing of the Photon with Low Mass Particles*, *Phys. Rev. D* **37** (1988) 1237.
- [78] E. Lopez-Rodriguez, J. A. Guerra, M. Asgari-Targhi and J. T. Schmelz, *The strength and structure of the magnetic field in the galactic outflow of messier 82*, *The Astrophysical Journal* **914** (2021) 24.
- [79] F. R. Candón, D. F. G. Fiorillo, G. Lucente, E. Vitagliano and J. K. Vogel, *NuSTAR Bounds on Radiatively Decaying Particles from M82*, *Phys. Rev. Lett.* **134** (2025) 171004 [2412.03660].
- [80] D. Nelson, A. Pillepich, V. Springel, R. Pakmor, R. Weinberger, S. Genel, P. Torrey, M. Vogelsberger, F. Marinacci and L. Hernquist, *First Results from the TNG50 Simulation: Galactic outflows driven by supernovae and black hole feedback*, *Mon. Not. Roy. Astron. Soc.* **490** (2019) 3234 [1902.05554].
- [81] F. Marinacci et al., *First results from the IllustrisTNG simulations: radio haloes and magnetic fields*, *Mon. Not. Roy. Astron. Soc.* **480** (2018) 5113 [1707.03396].
- [82] M. Khademi, S. Nasiri and F. S. Tabatabaei, *Influence of magnetic fields on the gas rotation in the galaxy ngc 6946*, *The Astrophysical Journal* **945** (2023) 36.
- [83] M. Ehle and R. Beck, *Ionized gas and intrinsic magnetic fields in the spiral galaxy NGC 6946.*, *A&A* **273** (1993) 45.
- [84] D. Horns, L. Maccione, M. Meyer, A. Mirizzi, D. Montanino and M. Roncadelli, *Hardening of TeV gamma spectrum of AGNs in galaxy clusters by conversions of photons into axion-like particles*, *Phys. Rev. D* **86** (2012) 075024 [1207.0776].
- [85] PARTICLE DATA GROUP Collaboration, S. Navas et al., *Review of particle physics*, *Phys. Rev. D* **110** (2024) 030001.
- [86] G. J. Feldman and R. D. Cousins, *A Unified approach to the classical statistical analysis of small signals*, *Phys. Rev. D* **57** (1998) 3873 [physics/9711021].
- [87] K. Nakamura, S. Horiuchi, M. Tanaka, K. Hayama, T. Takiwaki and K. Kotake, *Multi-messenger signals from core-collapse supernovae*, *IAU Symp.* **329** (2016) 428.
- [88] R. C. Kennicutt, Jr., J. C. Lee, J. G. Funes S. J., S. Sakai and S. Akiyama, *An H-alpha Imaging Survey of Galaxies in the Local 11 Mpc Volume*, *Astrophys. J. Suppl.* **178** (2008) 247 [0807.2035].
- [89] R. B. Tully et al., *Cosmicflows-2: The Data*, *Astron. J.* **146** (2013) 86 [1307.7213].
- [90] F. Oehsenbein, P. Bauer and J. Marcout, *The VizieR database of astronomical catalogues*, *Astron. Astrophys. Suppl. Ser.* **143** (2000) 23 [astro-ph/0002122].
- [91] R. Arbour and T. Boles, *Supernova 2008S in NGC 6946*, *Central Bureau Electronic Telegrams* **1234** (2008) 1.
- [92] R. Mostardi, W. Li and A. V. Filippenko, *Possible Supernova in NGC 4490*, *Central Bureau Electronic*

- Telegrams* **1280** (2008) 1.
- [93] L. A. G. Monard, *Supernova 2008bk in NGC 7793*, *Central Bureau Electronic Telegrams* **1315** (2008) 1.
- [94] A. Brunthaler et al., *VLBI observations of SN 2008iz: I. Expansion velocity and limits on anisotropic expansion*, *Astron. Astrophys.* **516** (2010) A27 [1003.4665].
- [95] J. L. Prieto et al., *SN 2008jb: A 'Lost' Core-Collapse Supernova in a Star-Forming Dwarf Galaxy at ~ 10 Mpc*, *Astrophys. J.* **745** (2012) 70 [1107.5043].
- [96] S. Benetti, S. Valenti, A. Magazzu and A. Harutyunyan, *Supernova 2009H in NGC 1084*, *Central Bureau Electronic Telegrams* **1667** (2009) 1.
- [97] C. Inserra et al., *The bright Type IIP SN 2009bw, showing signs of interaction*, *Mon. Not. Roy. Astron. Soc.* **422** (2012) 1122 [1202.0659].
- [98] S. Immler, B. R. Russell and P. J. Brown, *Swift XRT Detection of Supernova 2009dd in X-Rays*, *The Astronomer's Telegram* **2106** (2009) 1.
- [99] H. Navasardyan and S. Benetti, *Supernova 2009em in NGC 157*, *Central Bureau Electronic Telegrams* **1806** (2009) 1.
- [100] R. J. Foley, *Supernova 2009gj in NGC 134*, *Central Bureau Electronic Telegrams* **1858** (2009) 1.
- [101] N. Elias-Rosa et al., *The Massive Progenitor of the Possible Type II-Linear Supernova 2009hd in Messier 66*, *Astrophys. J.* **742** (2011) 6 [1108.2645].
- [102] K. e. a. Takáts, *Sn 2009ib: a type ii-p supernova with an unusually long plateau*, *Monthly Notices of the Royal Astronomical Society* **450** (2015) 3137–3154.
- [103] J. M. Silverman, M. T. Kandrashoff and A. V. Filippenko, *Supernova 2009js in NGC 918*, *Central Bureau Electronic Telegrams* **1969** (2009) 2.
- [104] M. Fraser et al., *SN 2009md: Another faint supernova from a low mass progenitor*, *Mon. Not. Roy. Astron. Soc.* **417** (2011) 1417 [1011.6558].
- [105] L. Chomiuk and A. Soderberg, *Radio observations of SN 2010br*, *The Astronomer's Telegram* **2587** (2010) 1.
- [106] N. Morrell and M. Stritzinger, *Supernova 2011am in NGC 4219 = Psn J12162600-4319200*, *Central Bureau Electronic Telegrams* **2667** (2011) 1.
- [107] T. Griga, A. Marulla, A. Grenier, G. Sun, X. Gao, S. Lamotte Bailey, R. A. Koff, H. Mikuz, B. Dintinjana, J. M. Silverman, S. B. Cenko, A. V. Filippenko, W. Li, M. Yamanaka, R. Itoh, A. Arai, M. Nagashima and K. Kajiwara, *Supernova 2011dh in M51 = Psn J13303600+4706330*, *Central Bureau Electronic Telegrams* **2736** (2011) 1.
- [108] L. A. G. Monard, S. Valenti and S. Benetti, *Supernova 2011dq in NGC 337 = Psn J00594775-0734205*, *Central Bureau Electronic Telegrams* **2749** (2011) 1.
- [109] J. J. Eldridge, M. Fraser, S. J. Smartt, J. R. Maund and R. M. Crockett, *The death of massive stars - II. Observational constraints on the progenitors of type Ibc supernovae*, *Mon. Not. Roy. Astron. Soc.* **436** (2013) 774 [1301.1975].
- [110] L. A. G. Monard, D. Milisavljevic, R. Fesen, T. Pickering, E. Romero-Colmenero, M. Turatto, S. Benetti, A. Pastorello, S. Valenti, F. Bufano, L. Tomasella, S. Ryder, A. Soderberg, C. Stockdale, S. van Dyk, S. Immler, K. Weiler and N. Panagia, *Supernova 2011ja in NGC 4945 = Psn J13051112-4931270*, *Central Bureau Electronic Telegrams* **2946** (2011) 1.
- [111] Y. Cao, M. M. Kasliwal, G. Wallerstein, A. Ritchey and D. A. Howell, *Supernova 2012A in NGC 3239*, *Central Bureau Electronic Telegrams* **2975** (2012) 1.
- [112] P. Fagotti, A. Dimai, U. Quadri, L. Strabla, R. Girelli, A. Quadri, L. Fiorentino, J. Skvarc and G. Masi, *Supernova 2012aw in M95 = PSN J10435372+1140177.*, *Central Bureau Electronic Telegrams* **3054** (2012) 1.
- [113] G. H. Marion, D. Milisavljevic and J. Irwin, *Supernova 2012cc in NGC 4419 = PSN J12265681+1502455.*, *Central Bureau Electronic Telegrams* **3105** (2012) 2.
- [114] C. Barbarino, M. Dall'Orta, M. T. Botticella, M. D. Valle, L. Zampieri, J. R. Maund, M. L. Pumo, A. Jerkstrand, S. Benetti, N. Elias-Rosa, M. Fraser, A. Gal-Yam, M. Hamuy, C. Inserra, C. Knapic, A. P. LaCluyze, M. Molinaro, P. Ochner, A. Pastorello, G. Pignata, D. E. Reichart, C. Ries, A. Riffeser, B. Schmidt, M. Schmidt, R. Smareglia, S. J. Smartt, K. Smith, J. Sollerman, M. Sullivan, L. Tomasella, M. Turatto, S. Valenti, O. Yaron and D. Young, *Sn 2012ec: mass of the progenitor from pessto follow-up of the photospheric phase*, *Monthly Notices of the Royal Astronomical Society* **448** (2015) 2312–2331.
- [115] S. Nakano, T. Yusa, K. Yoshimoto, L. Tomasella, M. Turatto, A. Pastorello, P. Ochner, E. Cappellaro, K. Takaki, R. Itoh, I. Ueno, T. Urano, Y. Moritani, H. Akitaya, K. S. Kawabata and M. Yamanaka, *Supernova 2012fh in NGC 3344 = Psn J10433405+2453290*, *Central Bureau Electronic Telegrams* **3263** (2012) 1.
- [116] P. Blanchard, W. Zheng, S. B. Cenko, W. Li, A. V. Filippenko, J. Brimacombe, M. Martignoni, A. Cucchiara, S. Valenti, D. Sand, J. T. Parrent, M. L. Graham and D. A. Howell, *Supernova 2013ab in NGC 5669 = Psn J14324449+0953123*, *Central Bureau Electronic Telegrams* **3422** (2013) 1.
- [117] S. Nakano, M. Sugano, K. Kadota, S. Benetti, L. Tomasella, A. Pastorello, E. Cappellaro, M. Turatto and P. Ochner, *Supernova 2013am in M65 = Psn J11185695+1303494*, *Central Bureau Electronic Telegrams* **3440** (2013) 1.
- [118] K. Itagaki, T. Noguchi, S. Nakano, L. Elenin, I. Molotov, Y. Moritani, K. Takaki, K. S. Kawabata, H. Akitaya, N. Ebisuda, K. Kawaguchi, K. Mori, Y. Ohashi, I. Ueno, M. Sasada, M. Yamanaka, P. Ochner, L. Tomasella, A. Pastorello, S. Benetti, E. Cappellaro and M. Turatto, *Supernova 2013bu in NGC 7331 = Psn J22370217+3424052*, *Central Bureau Electronic Telegrams* **3498** (2013) 1.
- [119] F. Ciabattari, E. Mazzoni, S. Donati, G. Petroni, S. Foglia, G. Galli, S. B. Cenko, K. I. Clubb, W. Zheng, P. L. Kelly, A. V. Filippenko and S. D. Van Dyk, *Supernova 2013df in NGC 4414 = Psn J12262933+3113383*, *Central Bureau Electronic Telegrams* **3557** (2013) 1.
- [120] F. Carrasco, M. Hamuy, R. Antezana, L. Gonzalez, R. Cartier, F. Forster, S. Silva, R. Ramirez, G. Pignata, Y. Apostolovski, E. Paillas, S. Varela, F. Aros, B. Conuel, G. Folatelli, D. E. Reichart, J. B. Haislip, J. P. Moore, A. P. LaCluyze, J. Vinko, G. H. Marion, J. M. Silverman, J. C. Wheeler, T. Szalai and R. Quimby, *Supernova 2013dk in NGC 4038 = Psn J12015272-1852183*, *Central Bureau Electronic Telegrams* **3565** (2013) 1.

- [121] G. Cortini, J. Brimacombe, L. Tomasella, P. Ochner, A. Pastorello, S. Benetti, E. Cappellaro, M. Turatto, J. Farinato, T. Pursimo and M. Dennefeld, *Supernova 2013ee in NGC 3079 = Psn J10015683+5541440*, *Central Bureau Electronic Telegrams* **3597** (2013) 1.
- [122] F. Huang, X. Wang, J. Zhang, P. J. Brown, L. Zampieri, M. L. Pumo, T. Zhang, J. Chen, J. Mo and X. Zhao, *SN 2013ej in M74: A Luminous and Fast-declining Type II-P Supernova*, *Astrophys. J.* **807** (2015) 59 [1504.00446].
- [123] S. Nakano, S. Kiyota, G. Masi, F. Nocentini, P. Schmeer, J. J. Zhang and X. F. Wang, *Supernova 2013ge in NGC 3287 = Psn J10344846+2139419*, *Central Bureau Electronic Telegrams* **3701** (2013) 1.
- [124] H. Kim, W. Zheng, W. Li, A. V. Filippenko, S. B. Cenko, L. Le Guillou, M. Fleury, S. Baumont, P. F. Leget, C. Inserra, S. Smartt, K. Smith, D. Young, M. Sullivan, S. Taubenberger, S. Valenti, M. Fraser, O. Yaron, I. Manulis, A. Gal-Yam, C. Knapic, R. Smareglia, M. Molinaro, E. Y. Hsiao and J. L. Prieto, *Supernova 2014A in NGC 5054 = Psn J13165936-1637570*, *Central Bureau Electronic Telegrams* **3771** (2014) 1.
- [125] M. Kim, W. Zheng, W. Li, A. V. Filippenko, S. B. Cenko, R. Arbour, G. Masi, F. Nocentini, P. Schmeer, J. Zhang, X. Want, L. Tartaglia, A. Pastorello, S. Benetti, E. Cappellaro, L. Tomasella, P. Ochner, N. Elias-Rosa and M. Turatto, *Supernova 2014C in NGC 7331 = Psn J22370560+3424319*, *Central Bureau Electronic Telegrams* **3777** (2014) 1.
- [126] J. Zhang et al., *Optical Observations of the Young Type Ic Supernova SN 2014L in M99*, *Astrophys. J.* **863** (2018) 109 [1806.08477].
- [127] M. Argo, M. Perez-Torres, A. Alberdi, R. Beswick, J. Conway, N. Elias-Rosa, R. Herrero-Illana, R. Kotak, P. Lundqvist, S. Mattila, J. Marcaide, T. Muxlow, I. Marti-Vidal, N. Ramirez-Olivencia, C. Romero-Canizales, C. Stockdale and E. Varenus, *Radio Detection of SN 2014bc in NGC 4258 with eMERLIN*, *The Astronomer's Telegram* **6270** (2014) 1.
- [128] S. Kumar, W. Zheng, A. V. Filippenko, G. Masi, J. j. Zhang and X. f. Wang, *Supernova 2014bi in NGC 4096 = Psn J12060299+4729335*, *Central Bureau Electronic Telegrams* **3892** (2014) 1.
- [129] S. Nakano, K. Itagaki, T. Yusa, S. Howerton, N. Elias-Rosa, L. Tartaglia, E. Cappellaro, A. Pastorello, M. T. Botticella, C. Inserra, K. Maguire, S. Smartt, K. W. Smith, M. Sullivan, S. Valenti, O. Yaron, D. Young and I. Manulis, *Supernova 2014cx in NGC 337 = Psn J00594783-0734186*, *Central Bureau Electronic Telegrams* **3963** (2014) 1.
- [130] L. A. G. Monard, R. Kneip, J. Brimacombe, H. Sato, M. Childress, G. Zhou, R. Scalzo, F. Yuan, B. Zhang, A. Ruiter, I. Seitzzahl, B. Schmidt and B. Tucker, *Supernova 2014df in NGC 1448 = Psn J03442399-4440081*, *Central Bureau Electronic Telegrams* **3977** (2014) 1.
- [131] T. Yusa, D. Buczynski, T. Noguchi, S. Nakano, S. Kiyota, G. Masi, K. Ayani, R. J. Foley, W. Zheng, A. V. Filippenko and S. D. Van Dyk, *Supernova 2015G in NGC 6951 = Psn J20372558+6607115*, *Central Bureau Electronic Telegrams* **4087** (2015) 1.
- [132] G. Bock, B. J. Shappee, K. Z. Stanek, J. L. Prieto, C. S. Kochanek, T. W. S. Holoiien, J. S. Brown, D. Godoy-Rivera, U. Basu, D. Bersier, S. Dong, P. Chen, J. Brimacombe, G. Masi and S. Kiyota, *ASASSN-16at: Discovery of A Probable Nearby Supernova in UGC 08041*, *The Astronomer's Telegram* **8566** (2016) 1.
- [133] P. J. Brown, N. J. Landez and B. A. Beeny, *Swift/UVOT Observations of SN2016adj in NGC5128*, *The Astronomer's Telegram* **8662** (2016) 1.
- [134] J. Johansson, M. Magee, I. Bar and O. Yaron, *PESSTO Transient Classification Report for 2016-04-16*, *Transient Name Server Classification Report* **2016-296** (2016) 1.
- [135] G. Bock, S. Dong, C. S. Kochanek, K. Z. Stanek, J. S. Brown, T. W. S. Holoiien, D. Godoy-Rivera, U. Basu, B. J. Shappee, J. L. Prieto, D. Bersier, P. Chen and J. Brimacombe, *ASASSN-16fq: Discovery of A Probable Supernova in M66*, *The Astronomer's Telegram* **9091** (2016) 1.
- [136] M. Shahbandeh, A. Sarangi, T. Temim, T. Szalai, O. D. Fox, S. Tinyanont, E. Dwek, L. Dessart, A. V. Filippenko, T. G. Brink, R. J. Foley, J. Jencson, J. Pierel, S. Zsiros, A. Rest, W. Zheng, J. Andrews, G. C. Clayton, K. De, M. Engesser, S. Gezari, S. Gomez, S. Gonzaga, J. Johansson, M. Kasliwal, R. Lau, I. De Looze, A. Marston, D. Milisavljevic, R. O'Steen, M. Siebert, M. Skrutskie, N. Smith, L. Strolger, S. D. Van Dyk, Q. Wang, B. Williams, R. Williams, L. Xiao and Y. Yang, *JWST observations of dust reservoirs in type IIP supernovae 2004et and 2017eau*, *Monthly Notices of the Royal Astronomical Society* **523** (2023) 6048 [2301.10778].
- [137] J. Lyman, D. Homan, M. Magee and O. Yaron, *ePESSTO Transient Classification Report for 2017-08-17*, *Transient Name Server Classification Report* **2017-881** (2017) 1.
- [138] F. Onori, *NUTS Transient Classification Report for 2017-09-03*, *Transient Name Server Classification Report* **2017-964** (2017) 1.
- [139] R. Dastidar et al., *SN 2018is: A low-luminosity Type IIP supernova with narrow hydrogen emission lines at early phases*, *Astron. Astrophys.* **694** (2025) A260 [2501.01530].
- [140] W. V. Jacobson-Galán et al., *SN 2019ehk: A Double-Peaked Ca-rich Transient with Luminous X-ray Emission and Shock-Ionized Spectral Features*, *Astrophys. J.* **898** (2020) 166 [2005.01782].
- [141] M. R. Siebert, C. D. Kilpatrick, R. J. Foley and R. Cartier, *UCSC Transient Classification Report for 2020-01-09*, *Transient Name Server Classification Report* **2020-90** (2020) 1.
- [142] M. Kawabata, *Transient Classification Report for 2020-02-27*, *Transient Name Server Classification Report* **2020-657** (2020) 1.
- [143] E. Kundu, S. D. Ryder, M. D. Filipovic, G. Anderson, C. Stockdale, K. Maeda, M. Renaud and R. Kotak, *Radio observations of SN 2020zbu*, *The Astronomer's Telegram* **14226** (2020) 1.
- [144] M. Lundquist, J. Andrews, S. Valenti, D. J. Sand, S. Wyatt, R. Amaro, J. Jencson, Y. Dong, S. Davis and D. Janzen, *DLT40 Transient Classification Report for 2020-12-13*, *Transient Name Server Classification Report* **2020-3777** (2020) 1.
- [145] K. A. Bostroem, J. Andrews, D. J. Sand, S. Wyatt, M. Lundquist, J. Jencson, Y. Dong, D. Janzen,

- G. Hosseinzadeh, J. Pearson, S. Valenti and N. Retamal, *DLT40 Transient Classification Report for 2022-01-28, Transient Name Server Classification Report* **2022-233** (2022) 1.
- [146] J. Grzegorzec, *PSH Transient Classification Report for 2022-05-11, Transient Name Server Classification Report* **2022-1261** (2022) 1.
- [147] J. Bayer, H. Wang, S. Huber, C. Vogl, S. Taubenberger, S. Kressierer, M. G. Cudmani, A. Holas, S. Benetti, E. Cappellaro, A. Pastorello, A. Reguitti, L. Tomasella and G. Pignata, *Padova-Asiago Transient Classification Report for 2022-06-29, Transient Name Server Classification Report* **2022-1820** (2022) 1.
- [148] K. Hinds and D. Perley, *ZTF Transient Classification Report for 2022-08-12, Transient Name Server Classification Report* **2022-2308** (2022) 1.
- [149] C. Balcon, *Transient Classification Report for 2022-10-19, Transient Name Server Classification Report* **2022-3048** (2022) 1.
- [150] V. Karambelkar, *ZTF Transient Classification Report for 2023-05-01, Transient Name Server Classification Report* **2023-990** (2023) 1.
- [151] D. Perley and A. Gal-Yam, *Transient Classification Report for 2023-05-19, Transient Name Server Classification Report* **2023-1164** (2023) 1.
- [152] M. A. Tucker, *SCAT Transient Classification Report for 2023-07-17, Transient Name Server Classification Report* **2023-1699** (2023) 1.
- [153] C. Balcon, *Transient Classification Report for 2023-09-10, Transient Name Server Classification Report* **2023-2224** (2023) 1.
- [154] C. Balcon, *Transient Classification Report for 2023-10-31, Transient Name Server Classification Report* **2023-2786** (2023) 1.
- [155] C. Balcon, *Transient Classification Report for 2024-01-29, Transient Name Server Classification Report* **2024-284** (2024) 1.
- [156] J. E. Andrews, K. A. Bostroem, S. Valenti, D. J. Sand, S. Jha, M. Lundquist, E. Hoang, M. Shrestha, Y. Dong, D. Janzen, G. Hosseinzadeh, J. Pearson, N. Meza, D. Metha, A. Ravi and A. Martas, *DLT40 Transient Classification Report for 2024-07-12, Transient Name Server Classification Report* **2024-2403** (2024) 1.
- [157] K. A. Bostroem, R. Kyer, J. Strader, M. Shrestha, M. Newsome, G. Terreran, C. McCully, D. J. Sand, S. Jha, J. E. Andrews, S. Valenti, M. Lundquist, E. Hoang, Y. Dong, D. Janzen, G. Hosseinzadeh, J. Pearson, N. Meza, D. Metha, A. Ravi, A. Martas, D. A. Howell, M. Andrews, J. Farah and E. P. Gonzalez, *DLT40 Transient Classification Report for 2024-07-24, Transient Name Server Classification Report* **2024-2571** (2024) 1.
- [158] W. Hoogendam, *SCAT Transient Classification Report for 2025-06-18, Transient Name Server Classification Report* **2025-2281** (2025) 1.
- [159] J. Strader, *Transient Classification Report for 2025-07-03, Transient Name Server Classification Report* **2025-2547** (2025) 1.
- [160] M. Hempel and J. Schaffner-Bielich, *Statistical Model for a Complete Supernova Equation of State*, *Nucl. Phys. A* **837** (2010) 210 [0911.4073].
- [161] A. W. Steiner, M. Hempel and T. Fischer, *Core-collapse supernova equations of state based on neutron star observations*, *Astrophys. J.* **774** (2013) 17 [1207.2184].
- [162] T. Sukhbold, S. Woosley and A. Heger, *A High-resolution Study of Presupernova Core Structure*, *Astrophys. J.* **860** (2018) 93 [1710.03243].
- [163] D. Nelson et al., *The IllustrisTNG simulations: public data release*, *Comput. Astrophys. Cosmol.* **6** (2019) 2 [1812.05609].
- [164] M. A. Lara-López, L. S. Pilyugin, J. Zaragoza-Cardiel, I. A. Zinchenko, O. López-Cruz, S. P. O’Sullivan, M. E. De Rossi, S. Dib, L. E. Garduño, M. Rosado, M. Sánchez-Cruces and M. Valerdi, *Metal-THINGS: Association and optical characterization of supernova remnants with H I holes in NGC 6946*, *A&A* **669** (2023) A25 [2210.11878].
- [165] D. Tran, B. Williams, E. Levesque, M. Lazzarini, J. Dalcanton, A. Dolphin, B. Koplitz, A. Smercina and O. G. Telford, *Spatially-resolved recent star formation history in ngc 6946*, 2023.
- [166] FERMI-LAT Collaboration, P. Bruel, T. H. Burnett, S. W. Digel, G. Johannesson, N. Omodei and M. Wood, *Fermi-LAT improved Pass 8 event selection*, in *8th International Fermi Symposium: Celebrating 10 Year of Fermi*, 10, 2018, 1810.11394.
- [167] FERMI-LAT Collaboration, W. Atwood et al., *Pass 8: Toward the Full Realization of the Fermi-LAT Scientific Potential*, 3, 2013, 1303.3514.
- [168] Fermi Science Support Center / NASA Goddard Space Flight Center, *LAT Specifications & Performance*, <https://fermi.gsfc.nasa.gov/science/instruments/table1-1.html>. Accessed: 24 Nov 2025.
- [169] Fermi Science Support Center, *Fermi LAT Background Models*, <https://fermi.gsfc.nasa.gov/ssc/data/access/lat/BackgroundModels.html>. Accessed: 12 Feb 2025.
- [170] FERMI-LAT Collaboration, W. B. Atwood et al., *The Large Area Telescope on the Fermi Gamma-ray Space Telescope Mission*, *Astrophys. J.* **697** (2009) 1071 [0902.1089].
- [171] B. Fore and S. Reddy, *Pions in hot dense matter and their astrophysical implications*, *Phys. Rev. C* **101** (2020) 035809 [1911.02632].
- [172] B. Fore, N. Kaiser, S. Reddy and N. C. Warrington, *Mass of charged pions in neutron-star matter*, *Phys. Rev. C* **110** (2024) 025803 [2301.07226].
- [173] D. A. Dicus, E. W. Kolb, V. L. Teplitz and R. V. Wagoner, *Astrophysical Bounds on the Masses of Axions and Higgs Particles*, *Phys. Rev. D* **18** (1978) 1829.
- [174] G. G. Raffelt, *Astrophysical axion bounds diminished by screening effects*, *Phys. Rev. D* **33** (1986) 897.

Supplemental Material for the Letter

Detecting light axions from supernovae in nearby galaxies

In the Supplemental Material (SM), we present the supernova catalog used in our analysis, provide fitting formulas for axion production in the supernova core, describe the models adopted for magnetic fields in the various astrophysical environments considered, and discuss details of the computation of the sensitivities reported in the main text, as well as potential sources of uncertainty affecting them. We also compare our results with previous literature.

A. Supernova catalog

In Table S1 we present the list of supernovae (SNe) employed in our analysis taken from the Transient Name Server catalog [62]. We include only SNe that are unambiguously identified as core-collapse events and that occurred during the *Fermi*-LAT operational period (2008–2025). In the spirit of this work, the goal here is to estimate how many SN events in the nearby Universe can be detected with current facilities over the typical lifetime of a gamma-ray mission. In the Table, we also quote the distances of the galaxies hosting the SN event. Following Ref. [87], we use the catalog in Ref. [88] for distances $\lesssim 10$ Mpc. For host galaxies at distances $d \gtrsim 10$ Mpc, we refer to Ref. [89] by employing the interface provided by Ref. [90].

TABLE S1: List of observed core-collapse SNe between 2008 and 2025 taken from the Transient Name Server catalog [62]. The Table reports the supernova name, SN type, distance (in Mpc), name of the host galaxy, and the references confirming each event. We use the SN distances reported in Ref. [88] for host galaxies at $d \lesssim 10$ Mpc and Ref. [90] for $d \gtrsim 10$ Mpc.

Name	Type	Distance (Mpc)	Host Galaxy	References
SN 2008S	SN IIn	5.9	NGC6946	[91]
SN 2008ax	SN IIP	8.0	NGC4490	[92]
SN 2008bk	SN IIP	3.91	NGC 7793	[93]
SN 2008iz	SN II	3.53	NGC 3034	[94]
SN 2008jb	SN II	9.6	ESO 302-14	[95]
SN 2009H	SN II	20.89	NGC 1084	[96]
SN 2009bw	SN II	9.46	UGC 2890	[97]
SN 2009dd	SN II	14.45	NGC4088	[98]
SN 2009em	SN Ic	12.08	NGC 157	[99]
SN 2009gj	SN I Ib	19.95	NGC 134	[100]
SN 2009hd	SN II	10.05	NGC 3627	[101]
SN 2009ib	SN IIP	12.59	NGC 1559	[102]
SN 2009js	SN II	15.92	NGC 918	[103]
SN 2009md	SN II	20.8	NGC 3389	[104]
SN 2010br	SN I b/c	11.02	NGC 4051	[105]
SN 2011am	SN Ib	20.2	NGC 4219	[106]
SN 2011dh	SN IIP	8.0	NGC 5194	[107]
SN 2011dq	SN II	18.88	NGC 337	[108]
SN 2011hp	SN Ic	20.2	NGC 4219	[109]
2011ja	SN IIP	3.6	NGC 4945	[110]
SN 2012A	SN II	8.3	NGC 3239	[111]
SN 2012aw	SN IIP	10.0	NGC 3351	[112]

Name	Type	Distance (Mpc)	Host Galaxy	References
SN 2012cc	SN II	13.49	NGC 4419	[113]
SN 2012ec	SN IIP	20.89	NGC 1084	[114]
SN 2012fh	SN Ib/c	6.6	NGC3344	[115]
SN 2013ab	SN II	15.630	NGC 5669	[116]
SN 2013am	SN IIP	8.9	M65	[117]
SN 2013bu	SN II	13.87	NGC 7331	[118]
SN 2013df	SN II	17.86	NGC 4414	[119]
SN 2013dk	SN Ic	20.610	NGC 4038	[120]
SN 2013ee	SN II	20.610	NGC 3079	[121]
SN 2013ej	SN II	7.3	NGC 628	[122]
SN 2013ge	SN Ib	14.79	NGC 3287	[123]
SN 2014A	SN II	18.2	NGC 5054	[124]
SN 2014C	SN Ib	13.87	NGC 7331	[125]
SN 2014L	SN Ic	13.870	NGC 4254	[126]
SN 2014bc	SN IIP	7.98	NGC 4258	[127]
SN 2014bi	SN II	8.3	NGC 4069	[128]
SN 2014cx	SN II	18.88	NGC 337	[129]
SN 2014df	SN Ib	17.22	NGC 1448	[130]
SN 2015G	SN Ibn	18.79	NGC 6951	[131]
SN 2016X	SN IIP	14.45	UGC 08041	[132]
SN 2016adj	SN I Ib	3.6	NGC 5128	[133]
SN 2016bmi	SN IIP	19.77	IC4721	[134]
SN 2016cok	SN IIP	10.05	NGC 3627	[135]
SN 2016ija	SN II	20.04	NGC1532	[64]
SN 2017eaw	SN IIP	5.9	NGC 6946	[136]
SN 2017gaw	SN II	16.9	UGC807	[137]
SN 2017gkk	SN I Ib	19.77	NGC2748	[138]
SN 2018is	SN II	18.2	NGC 5054	[139]
SN 2019ehk	SN Ib	13.93	NGC 4321	[140]
SN 2020oi	SN Ic	13.93	NGC 4321	[141]
SN 2020dpw	SN IIP	18.79	NGC 6952	[142]
SN 2020zbv	SN IIP	17.22	NGC1448	[143]
SN 2020acli	SN IIIn-pec	2.0	NGC 300	[144]
SN 2022ame	SN II	13.61	NGC 1255	[145]
SN 2022jli	SN Ic	12.08	NGC 157	[146]
SN 2022myz	SN I	20.14	NGC 4217	[147]
SN 2022oey	SN II	14.39	UGC 02855	[148]
SN 2022xxf	SN Ic-BL	19.14	NGC 3705	[149]
SN 2023hlf	SN II	17.86	NGC 4414	[150]
SN 2023ixf	SN II	16.95	NGC 545	[151]

Name	Type	Distance (Mpc)	Host Galaxy	References
SN 2023mut	SN I Ib	8.1	UGC 03174	[152]
SN 2023rve	SN II	16.0	NGC 1097	[153]
SN 2023wcr	SN II	14.06	NGC4346	[154]
SN 2024bch	SN II	18.11	NGC 3206	[155]
SN 2024phv	SN II	19.23	NGC 3969	[156]
SN 2024pxg	SN II	12.36	NGC6221	[157]
SN 2025nqb	SN Ib	14.72	NGC 4496B	[158]
SN 2025pht	SN I IP	17.46	NGC 1637	[159]

B. SN ALP spectrum

In this work we calculate the SN ALP fluxes using as benchmark the 1D spherical symmetric GARCHING group's SN model SFHo-s18.8 provided in Ref. [74] and based on the neutrino-hydrodynamics code PROMETHEUS-VERTEX [75]. The simulation employs the SFHo Equation of State (EoS) [160, 161] and is launched from a stellar progenitor with mass $18.8 M_\odot$ [162], leading to neutron star (NS) with baryonic mass $1.35 M_\odot$. This model corresponds to the cold model used in Refs. [45, 46], leading to the most conservative results. We consider SN ALP production via the Lagrangian

$$\mathcal{L}_{aN} = \frac{\partial_\mu a}{2m_N} \sum_{N=p,n} g_{aN} \bar{N} \gamma^\mu \gamma_5 N, \quad (\text{S1})$$

from both nucleon-nucleon bremsstrahlung (NN) and Compton pionic processes (πN). In order to characterize the resulting SN ALP spectra, we integrated in time the spectra used in Ref. [53] from the SFHo-s18.8 model, in the time window [1;8] seconds. For the time-integrated spectra we provide as analytical fit for the bremsstrahlung production

$$\frac{dN}{dE} = C \left(\frac{g_{ap}}{10^{-9}} \right)^2 \left(\frac{E}{E_0} \right)^\beta \exp \left[-\frac{(\beta+1)E}{E_0} \right], \quad (\text{S2})$$

with $C = 1.22 \times 10^{55} \text{ MeV}^{-1}$, $E_0 = 67.7 \text{ MeV}$, and $\beta = 1.3$. The NN spectrum computed here includes all the corrections discussed in Refs. [39]. Similar results would be obtained using the parametric treatment proposed by Ref. [46], where all nuclear uncertainties are encoded in the nucleon spin-flip rate, which is quite consistent with Ref. [39].

Conversely, if pions are present in the SN core, the resulting time-integrated spectrum for the Compton pionic processes is given by

$$\frac{dN}{dE} = C_\pi \left(\frac{g_{ap}}{10^{-9}} \right)^2 \left(\frac{E - \omega_c}{E_{0\pi}} \right)^{\beta_\pi} \exp \left[-\frac{(\beta_\pi+1)(E - \omega_c)}{E_{0\pi}} \right], \quad (\text{S3})$$

with $C_\pi = 4.08 \times 10^{54} \text{ MeV}^{-1}$, $E_{0\pi} = 115.8 \text{ MeV}$, $\beta_\pi = 1.15$, and $\omega_c = 99.1 \text{ MeV}$. The total spectrum with these two components is shown in Fig. S1.

C. Magnetic fields in host galaxies and conversion probabilities

In this analysis, we employ publicly available simulation data from the ILLUSTRISTNG project to model the magnetic field and the electron number density of the three galaxies under study, namely M82, NGC 6946, M87 [163]. The ILLUSTRISTNG project consists of a series of cosmological magnetohydrodynamical simulations of galaxy formation, which also aims to provide predictions for both current and future observational programs. For the environments investigated in this work, we used data from different simulation volumes, selecting in each case the highest space

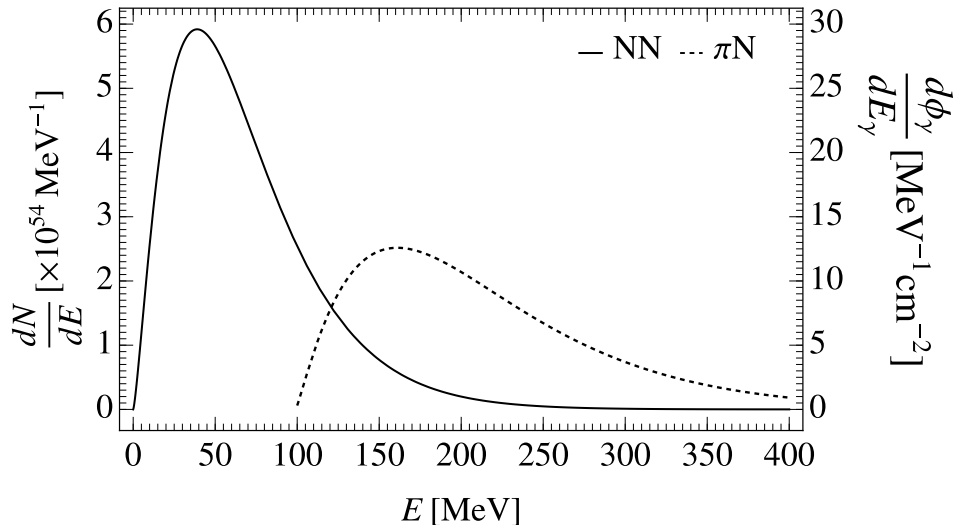


FIG. S1. Time-integrated ALP emission spectrum from NN bremsstrahlung (solid line), and pionic processes (dashed line). These spectra are obtained from fitting formulas in Eqs. (S2) and (S3) by setting $g_{ap} = 10^{-9}$ and $g_{an} = 0$. On the right axis the corresponding values of the photon flux from M82 reaching the Earth by considering ALP–photon conversion in the subhalo and along the line of sight that yield the average conversion probability. The ALP–photon conversion probability is estimated at $g_{a\gamma} = 10^{-12} \text{ GeV}^{-1}$.

resolution realizations available. The subhalos included in our analysis were identified by searching for candidates capable of reproducing the observed total stellar mass and star-formation rate (SFR) of the three galaxies, following Ref. [49]. The relevant properties of the selected subhalos for the three environments are reported in Table S2. We highlight that the selected subhalos present physical extensions consistent with those of the corresponding host environments.

For each subhalo, we compute the conversion probabilities $P_{a\gamma}$ by solving the beam propagation equation, closely following the method of Ref. [84], assuming that ALPs are produced in a SN at the center of the host galaxy. In Fig. S3 we show the histograms of the conversion probability distributions along 1000 random directions obtained for each given subhalo employed for M82 (upper panel), NGC 6946 (middle panel) and M87 (lower panel). In absence of a detailed model of the SN expected distributions in the considered host galaxies, we assume all the SNe located in the center of the host galaxy. We adopt the average probability of each distribution, indicated by an arrow in Fig. S3 and listed in Table S3, to compute the sensitivities shown in Fig. 1. We define the line of sight associated to this average conversion probability as our *fiducial* line of sight. For illustrative purposes, in Fig. S2 we show the profile of the transverse magnetic field B_T and free-electron density n_e along our fiducial line of sight for M82 (left panel, solid line), for NGC 6946 (left panel, dashed line) and for Virgo Cluster (right panel, solid line). We highlight that the structure of the magnetic field assumed for M82 is subject to sudden variations over correlation lengths shorter than NGC 6946. Thus, although the larger dimension of the assumed M82 subhalo, we expect the conversion probabilities to lose coherence at slightly higher ALP masses than NGC 6946 (see Fig. 1).

Moreover, in order to characterize the uncertainties in the conversion probability due to the unknown orientation of the line of sight, we assume as ranges of $P_{a\gamma}$ the ones determined by selecting the percentiles that enclose 68% and 95% of the realizations around the central probability values. These intervals are then used to determine the uncertainty bands for the sensitivities to the ALP parameters shown in the following (See SM E).

To assess the validity of the ILLUSTRISTNG simulation results in the characterization of the magnetic fields of the considered astrophysical environments, we compare our results for the case of NGC 6946 with the ones obtained using the magnetic field model presented in Ref. [82], which consists of a spiral component confined to the galactic plane and an X-shaped poloidal component. However, since no explicit model or numerical values are provided for the X-shaped component, only the spiral magnetic field was included in our analysis. This model features a minor uncertainty associated with the maximum field strength along the spiral arms, which can vary between $8 \mu\text{G}$ and $10 \mu\text{G}$. To model the electron number density, the average values of n_e reported in Ref. [83] are adopted (Tab. 8, model 3). Using these inputs, the conversion probability in the massless regime is found to be $P_{a\gamma} = 6.8 \times 10^{-3}$, approximately

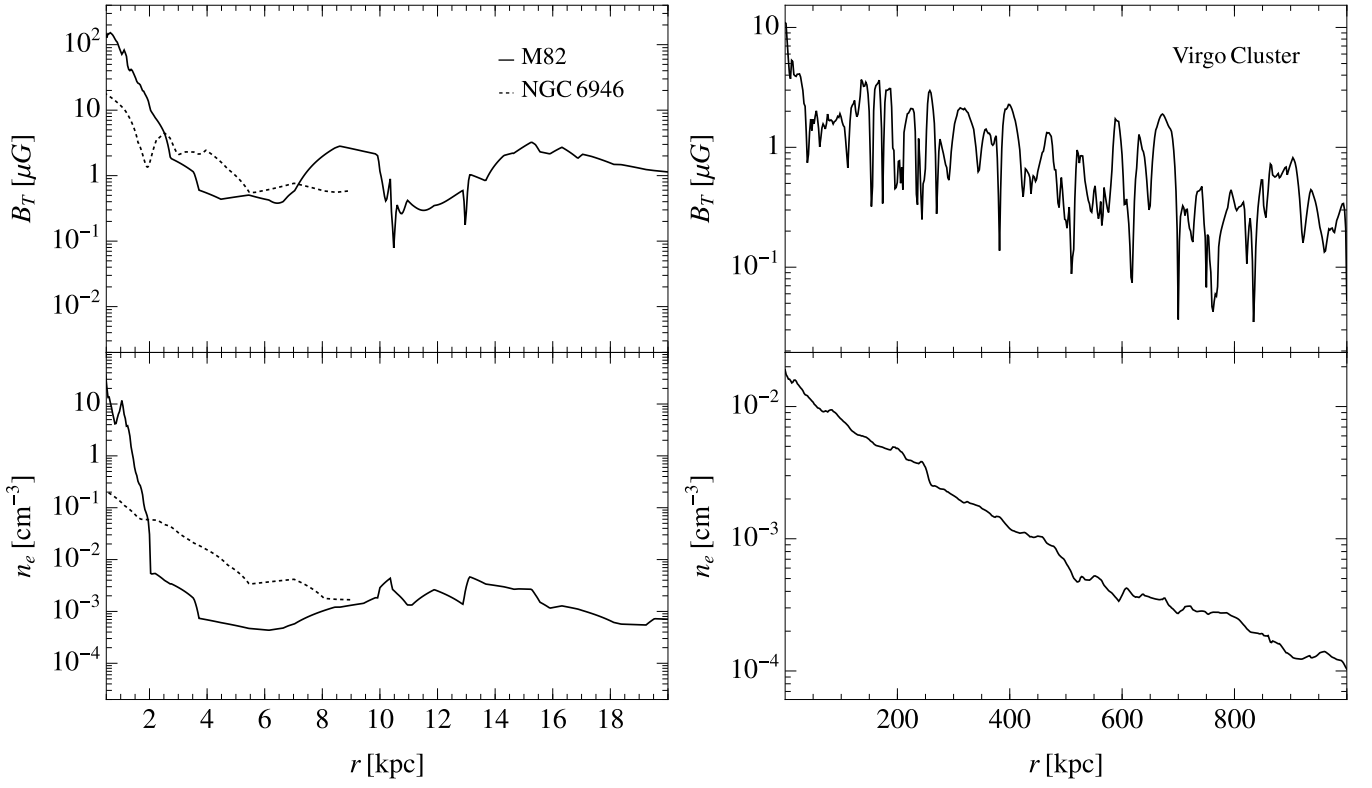


FIG. S2. Magnetic-field profiles (upper panels) and free-electron density profiles n_e (lower panels) as a function of the distance from the galactic center for our fiducial line of sight. The left panel refers to M82 (solid line) and NGC 6946 (dashed line), while results for the Virgo Cluster are reported in the right panel.

TABLE S2. Summary of the ILLUSTRITNG profiles used in this work. For each host galaxy, the Table lists the total stellar mass, the star-formation rate (SFR), the corresponding ILLUSTRITNG simulation volume, and the identifiers of the subhalos that best reproduce the observed properties of the respective environments.

Host environment	Total stellar mass (M_\odot)	SFR ($M_\odot \text{ yr}^{-1}$)	Simulation volume	Subhalos
M82	$\sim 10^{10}$ [49]	~ 10 [49]	50	167408, 300907, 544408
NGC 6946	$\sim 10^{10.5}$ [164]	~ 5 [165]	100	227576
Virgo Cluster	$\sim 10^{14}$ [49]	–	300	42631, 47315, 55060, 58081, 61682, 64929, 701461

a factor of 1.7 smaller than the value reported in Table S3, obtained using ILLUSTRITNG. The resulting change in the sensitivity on $g_{ap} \times g_{a\gamma}$ would be weaker by only a factor 1.3, consolidating the robustness of our results.

To gain some physical intuition, it is also useful to study approximate analytical solutions. As shown in Ref. [52], in the massless case the conversion probability becomes energy independent, and for $\Delta_{a\gamma} L < 1$ reduces to

$$P_{a\gamma} \simeq (\Delta_{a\gamma} L)^2, \quad (\text{S4})$$

where L is the size of the magnetic domain, and

$$\Delta_{a\gamma} \simeq 1.5 \times 10^{-3} \left(\frac{g_{a\gamma}}{10^{-12} \text{ GeV}^{-1}} \right) \left(\frac{\langle B_T \rangle}{10^{-6} \text{ G}} \right) \text{ kpc}^{-1}, \quad (\text{S5})$$

with $\langle B_T \rangle$ the average of the transverse component of the magnetic field along the line of sight. For an ALP moving

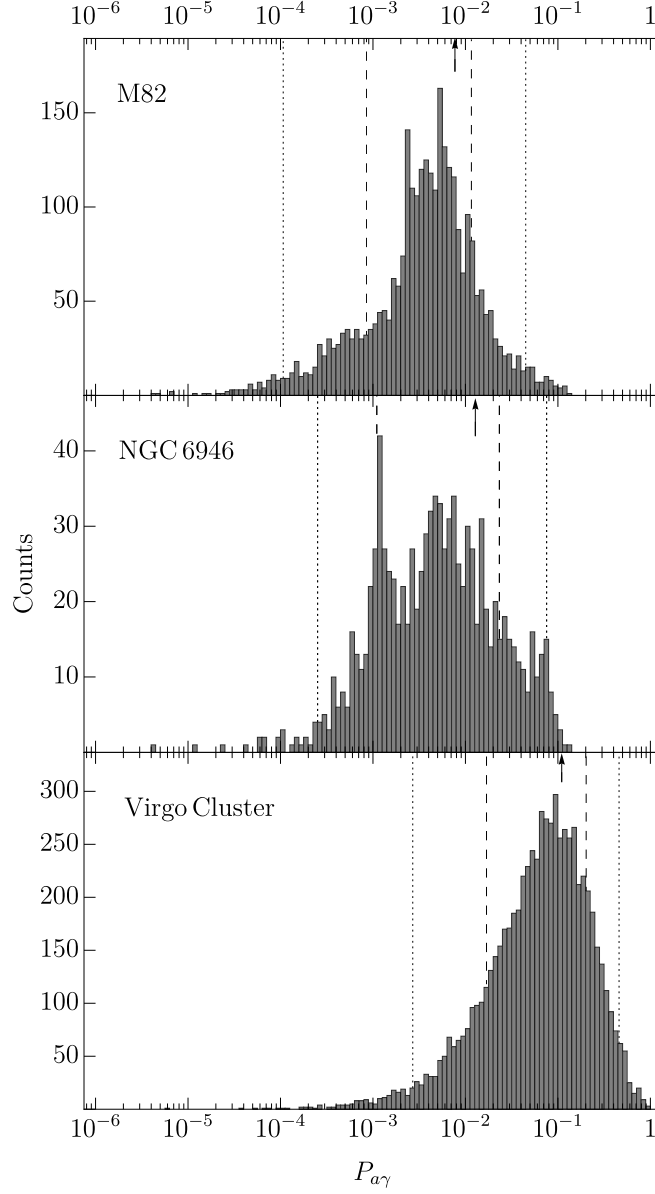


FIG. S3. Distribution of conversion probabilities along 1000 randomly distributed lines of sight within the various subhalo models for M82 (upper panel), NGC 6946 (middle panel) and Virgo Cluster (lower panel). These results are obtained by assuming $g_{a\gamma} = 10^{-12} \text{ GeV}^{-1}$ and $m_a \lesssim 10^{-10} \text{ eV}$. The arrow indicates the average value of the probabilities. The dashed (dotted) lines indicate the percentile intervals enclosing 68% (95%) of the values around the central value.

in the z direction, this is given by

$$\langle B_T \rangle = \frac{1}{L} \sqrt{\left| \int_0^L dz B_x(z) \right|^2 + \left| \int_0^L dz B_y(z) \right|^2}. \quad (\text{S6})$$

The values of the parameters entering Eq. (S4) for the three considered galaxies are reported in Table S3. In the massless limit ($m_a \ll 10^{-9} \text{ eV}$), the probability from Eq. (S4) reported in Tab. S3 agrees with the result obtained using the method of Ref. [84].

TABLE S3. Observed supernovae for the period 2008–2025 in M82, NGC 6946 and in Virgo Cluster. The table reports also the average transverse magnetic field $\langle B_T \rangle$ along the fiducial line of sight, the extension of the host environment L , its distance from Earth d , the average ALP-photon conversion probability $P_{a\gamma}$ for massless ALPs with $g_{a\gamma} = 10^{-12} \text{ GeV}^{-1}$, and the sensitivity to $g_{ap} \times g_{a\gamma}$ in the massless case.

Host	Observed SNe	$\langle B_T \rangle$	L	d	$P_{a\gamma}$	$g_{ap} \times g_{a\gamma}$
Environment	(2008-2025)	(μG)	(kpc)	(Mpc)		($\times 10^{-25} \text{ GeV}^{-1}$)
M82	SN 2008iz	2.9	20	3.5	7.7×10^{-3}	7.3
NGC 6946	SN 2008S, SN 2017eaw	8.3	9	5.9	1.2×10^{-2}	9.5
Virgo Cluster	SN 2012cc, SN 2014L, SN 2020oi, SN 2019ehk	0.2	10^3	16.4	1.1×10^{-1}	9.1

D. Sensitivities in ALP-induced gamma-ray signals

We characterize the detectability of a gamma-ray burst induced by SN ALP conversions, assuming a telescope with the same performances of *Fermi*-LAT [166]. We compute the number of expected gamma-ray events as

$$N_{\text{ev}} = \int_{E_{\text{min}}}^{E_{\text{max}}} dE \frac{d\phi_{\gamma}}{dE} A_{\text{eff}}(E), \quad (\text{S7})$$

where $d\phi_{\gamma}/dE$ is the ALP-induced photon flux reaching the Earth, A_{eff} is the *Fermi*-LAT effective area, and $[E_{\text{min}}, E_{\text{max}}] = [60, 250] \text{ MeV}$ is our considered energy window, above the energy threshold of *Fermi*-LAT. The photon flux produced by ALP-photon conversion in the host galaxy magnetic field and reaching the Earth is given by

$$\frac{d\phi_{\gamma}}{dE}(E, L) = \frac{1}{4\pi d^2} \frac{dN}{dE}(E) P_{a\gamma}(E, L), \quad (\text{S8})$$

where dN/dE is the ALP production spectrum (see SM B), $P_{a\gamma}(E, L)$ is the ALP–photon conversion probability, and d is the distance to the host galaxy (fifth column of Table S3). The resulting photon flux from M82 for $g_{a\gamma} = 10^{-12} \text{ GeV}^{-1}$ is shown in Fig. S1. The effective area $A_{\text{eff}}(E)$ used in this analysis is the one of *Fermi*-LAT for normal incident photons [166] (see Fig. S4). It is reasonable to use the on-axis effective area, as GALAXIS’ all sky coverage implies that most photons arrive with small incident angles. Moreover, Ref. [167] shows that the incident angle has only a minor impact on the effective area [54]. In order to describe the emission from the background sources and to extract the expected sensitivity from a given SN, one should derive a model for a region of interest (see Ref. [56]). In our simplified analysis we assume that we are able to extract the gamma-ray emission signal from this region and therefore we compare the ALP-induced signal with the only diffuse gamma-ray background. Then, the background event rate is computed as

$$R_{\text{bkg}} = \Omega \times \int_{E_{\text{min}}}^{E_{\text{max}}} dE \frac{d\phi_{\gamma, \text{bkg}}}{dE} A_{\text{eff}}(E), \quad (\text{S9})$$

where

$$\Omega = 2\pi (1 - \cos \delta\theta), \quad (\text{S10})$$

is the solid angle corresponding to the angular resolution $\delta\theta$. For our analysis we adopt an angular resolution of 3.5° [168]. The quantity $d\phi_{\gamma, \text{bkg}}/dE$ is the diffuse gamma-ray background reported in `iso_P8R3_SOURCE_V3_v1.txt` from Ref. [169]. The resulting background event rate is $R_{\text{bkg}} = 7.7 \times 10^{-4} \text{ s}^{-1}$. The number of background events is then $N_{\text{bkg}} = R_{\text{bkg}} \times \Delta t$, with Δt the observation time window. We consider three cases, namely $\Delta t = 1 \text{ d}$ and $\Delta t = 1 \text{ h}$, determined by the accuracy in the determination of the SN core-collapse time provided by optical survey, as well as $\Delta t = 10 \text{ s}$, corresponding to the ALP burst duration. The latter can be adopted only if a GW trigger determines the core-collapse time.

We find $N_{\text{bkg}} \simeq 67$ for $\Delta t = 1 \text{ d}$, indicating a relatively large background compared with the ALP-induced gamma-ray expected for the explored couplings. Following the procedure described in Ref. [85], under these conditions we evaluate the 95% CL sensitivity as

$$N_{\text{ev}} > 1.64 \sqrt{N_{\text{bkg}}}. \quad (\text{S11})$$

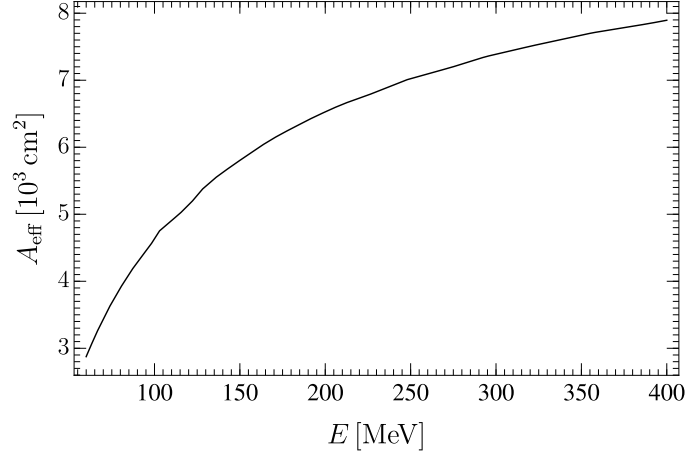


FIG. S4. On-axis effective area of *Fermi*-LAT for transient events (dotted curve in Fig. 14 of Ref. [170]).

For $\Delta t = 1$ h we find $N_{\text{bkg}} \simeq 3$, while for $\Delta t = 10$ s we obtain $N_{\text{bkg}} \simeq 0$, corresponding to a low-background and free background regime, respectively. In these situations, we adopt the Feldman–Cousins prescription [86], which is appropriate for the low-count limit. For these values of the background events, the 95% CL sensitivity corresponds to requiring $N_{\text{ev}} \gtrsim 5$ for $\Delta t = 1$ h, and $N_{\text{ev}} \gtrsim 3$ for $\Delta t = 10$ s [86].

If multiple SN explosions are observed, the combined (stacked) analysis improves the sensitivity to the product $g_{ap} \times g_{a\gamma}$. Since both the signal and background scale linearly with the number of stacked SNe N_{SN} , in the background-dominated regime we require the signal to background ratio to satisfy

$$N_{\text{SN}} N_{\text{ev}} > 1.64 \sqrt{N_{\text{SN}} N_{\text{bkg}}}. \quad (\text{S12})$$

Since $N_{\text{ev}} \propto g_{ap}^2 \times g_{a\gamma}^2$, the sensitivity scales as

$$g_{ap} \times g_{a\gamma} \propto N_{\text{SN}}^{-1/4}. \quad (\text{S13})$$

For observations with $\Delta t = 10$ s the background remains smaller than one event for $N_{\text{SN}} \lesssim 200$. In this case only the number of events scales with the number of SNe, and the corresponding sensitivity behaves as

$$g_{ap} \times g_{a\gamma} \propto N_{\text{SN}}^{-1/2}. \quad (\text{S14})$$

Being in a low-background regime, for $\Delta t = 1$ h the 95% CL sensitivity is determined using the thresholds tabulated in Table XII of Ref. [86]. This results in a sensitivity scaling that lies between the background-dominated and background-free regimes.

E. Uncertainties in ALP-induced gamma-ray signals

The sensitivities on $g_{ap} \times g_{a\gamma}$ vs m_a shown in Fig. 1 are those obtained with our fiducial line of sight, i.e. using the subhalo and line of sight which yield the average value of the distributions presented before, and taking $\Delta t = 10$ s. As previously discussed, confidence intervals are also extracted. Figure S5 shows the resulting uncertainty band for M82, obtained by evaluating the sensitivities using the subhalos and lines of sight corresponding to the extrema of the confidence-level intervals 68% and 95%. Due to the large variability of magnetic field strengths along the different subhalo models and various line of sights considered in the analysis, the uncertainty bands over $g_{ap} \times g_{a\gamma}$ may extend over ~ 1 order of magnitude.

A further source of uncertainty arises from the inclusion of pions in the production mechanism. Indeed, the role of pions in supernova cores remains uncertain, as they are often omitted in SN models. Earlier virial-expansion studies suggested that could reach abundances comparable to muons, growing with density and potentially affecting axion production [72, 171]. However, more recent chiral-effective-theory calculations find strongly increased in-medium pion energies, which would suppress pion abundance [172] (see the discussion of Ref. [46]). In order to quantify the impact of pionic processes, in Fig. S6 we show how the sensitivity plot for M82 changes if one includes these latter. We find an increase in sensitivity due to presence of pion processes by a factor ~ 2 .

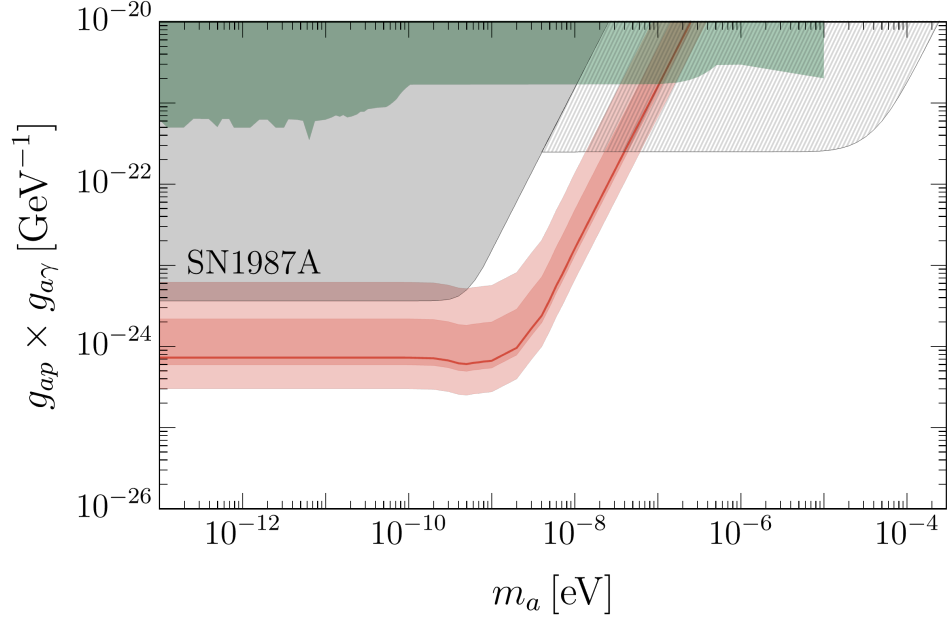


FIG. S5. Uncertainties in the sensitivity curves arising from the choice of line of sight in the ILLUSTRITNG subhalo models. Here we consider conversions in the M82 magnetic field as an exemplary case. The boundaries of the dark (light) red shaded band correspond to the lines of sight providing conversion probabilities enclosing the 68% (95%) percentile intervals around the mean value of the distribution shown in Fig. S3. The color scheme for other constraints is the same as the one used in Fig. 1.

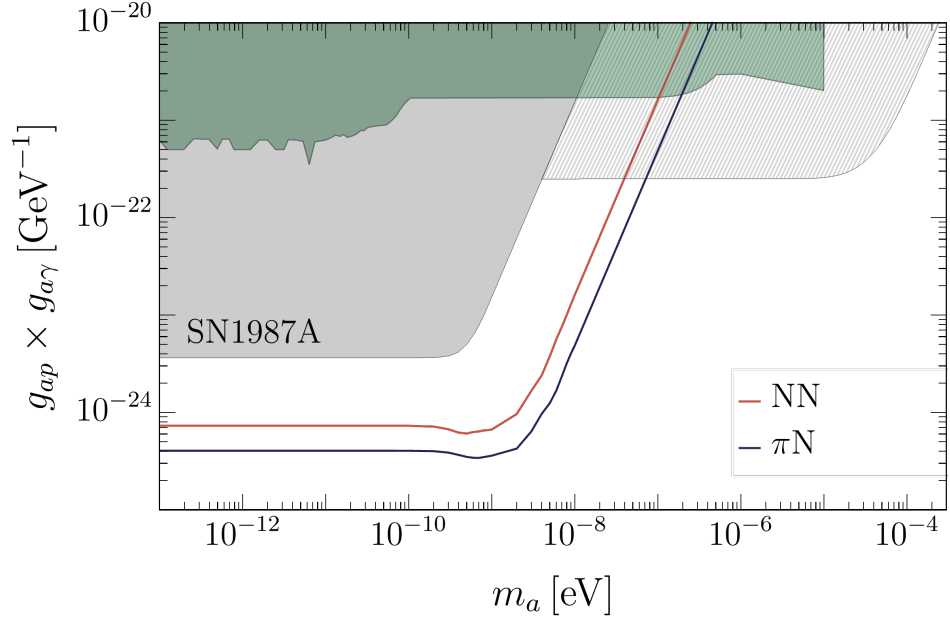


FIG. S6. Sensitivities at 95% CL for the fiducial M82 line of sight by considering ALP production via NN bremsstrahlung only (red) and by including also the contribution from pionic processes (blue). See text for details. The color scheme for other constraints is the same as the one used in Fig. 1.

F. ALPs coupling to photons only

Finally, in order to compare our results with previous literature [56], we consider the case of ALPs coupled with only photons and converting into gamma rays only in the Milky-Way magnetic field. We take as reference an extragalactic SN in M82. In case of only photon-ALP coupling, ALP would be produced in a SN core via Primakoff

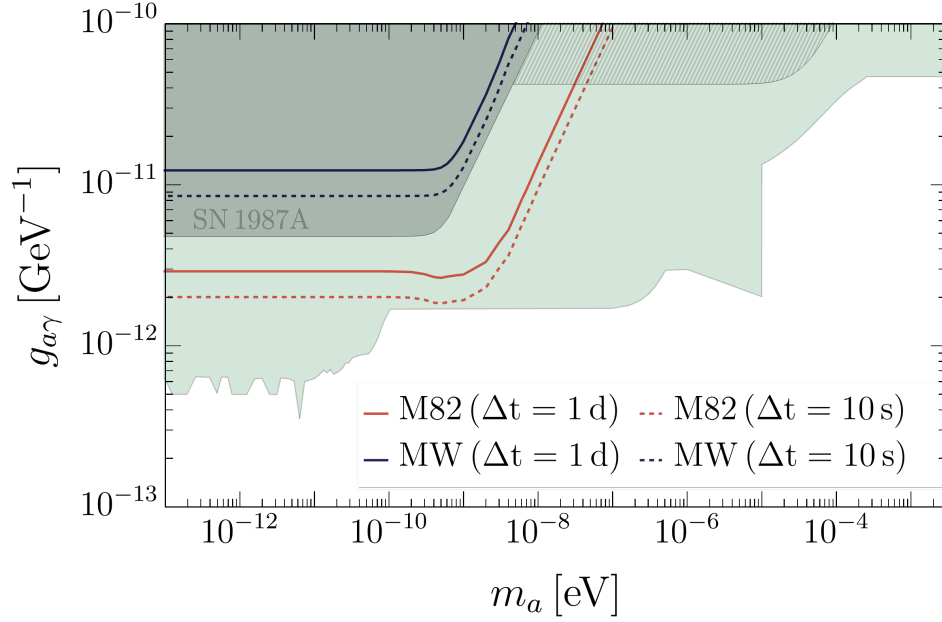


FIG. S7. Sensitivities at 95 % CL in the plane $g_{a\gamma}$ vs m_a for an extragalactic SN located in M82 assuming ALP-photon conversions in the Milky-Way (blue curves) and along a fiducial line of sight through the host-galaxy magnetic field (red curves). In this plot, we set ALP-nucleon $g_{aN} = 0$, so that ALP production in the SN core is triggered solely by the Primakoff process. Solid lines refer to $\Delta t = 1$ d and dashed lines to $\Delta t = 10$ s.

process [173, 174]. In this situation, we use as SN ALP flux the one presented in Ref. [46] for the one-zone model for a cold SN. We calculate ALP-photon conversions in the Milky Way following Ref. [52] and find $P_{a\gamma} \sim \mathcal{O}(10^{-5})$ for low-mass ALPs and $g_{a\gamma} = 10^{-12} \text{ GeV}^{-1}$. In Fig. S7, we show the 95% CL sensitivities in $g_{a\gamma}$ vs m_a plane for the situation described above, using an observation-time window $\Delta t = 1$ d. We find a sensitivity to $g_{a\gamma} \gtrsim 1.2 \times 10^{-11} \text{ GeV}^{-1}$ for $m_a \ll 10^{-9} \text{ eV}$, which is a factor ~ 2.5 worse in comparison with the corresponding SN 1987A bound. These results are consistent with those reported in Ref. [56]. For example, for SN 2017ein at a distance of $d \approx 11.6 \text{ Mpc}$ (see Fig. 1 of [56]), Ref. [56] obtained a bound of $2 \times 10^{-11} \text{ GeV}^{-1}$. After rescaling for the different distance assumed in our analysis ($d = 3.5 \text{ Mpc}$ for M82), this agrees well with our result. We realize that the improvement in the presence of $\Delta t = 10$ s is a factor 1.4. For comparison if we include also conversions in the magnetic field of the host environment we find a sensitivity to $g_{a\gamma} \gtrsim 3 \times 10^{-12} \text{ GeV}^{-1}$ for $\Delta t = 1$ d and $g_{a\gamma} \gtrsim 2 \times 10^{-12} \text{ GeV}^{-1}$ for $\Delta t = 10$ s, with an improvement of a factor 4 with respect to conversions in the only Milky-Way, but still excluded by other astrophysical constraints.